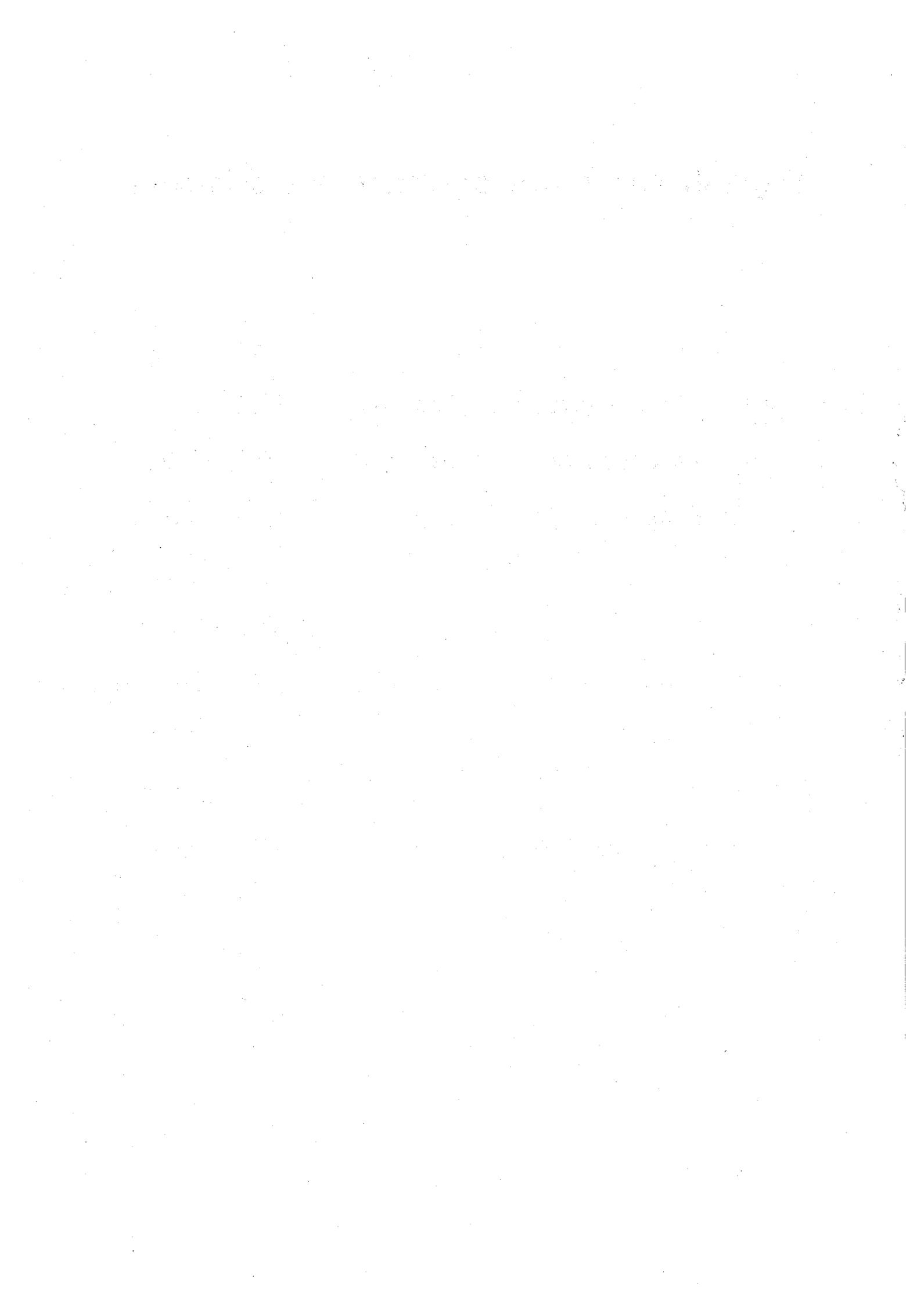


English Abstracts of Contributed Papers

Invitation Lecture :	(Sep.24)	2S01
Special Lectures :	(Sep.24)	2S02~2S04
Oral Presentations :	(Sep.23)	1A01~1A22
		1B01~1B23
		1C01~1C22
Oral Presentations :	(Sep.25)	3A01~3A07
		3B01~3B07
		3C01~3C08
Poster Presentations :	(Sep.25)	3P01~3P60



2S01: Synthesis and properties of superheavy elements

Hofmann, S. (GSI, Darmstadt, Germany)

In recent years the exploration of superheavy elements (SHE) received increasing interest both from theoretical as well as experimental investigation and both from chemical as well as physical studies. An overview of the facilities and identification methods presently used at GSI in Darmstadt, FLNR in Dubna and LBNL in Berkeley will be given. Results will be presented of recent studies of elements 110 to 112 measured at GSI in Darmstadt using cold fusion reactions.

2S02: Search for beneficial food materials produced in Hokkaido that helps to improve one's health –Using Senescence Accelerated Mouse (SAM) as an animal model of senescence – Okuma Y. (Dept. of Pharmacol., Grad. Sch. Pharmaceu. Sci., Hokkaido Univ.)

To elucidate the fundamental mechanism of age-related deficiencies and to develop effective drugs for intervention of age-related diseases such as learning dysfunctions, it is required to establish pertinent animal models that have characteristics closely similar to the human dysfunctions. SAM (senescence-accelerated mouse) has been established as a murine model of the SAM strains, groups of related inbred strains including nine strains of accelerated senescence-prone, short-lived mice (SAMP) and three strains of accelerated senescence-resistant, long-lived mice (SAMR). SAMP-strain mice show relatively strain-specific age-associated phenotypic pathologies such as shortened life span and early manifestation of senescence. Among SAMP-strain mice, SAMP8 and SAMP10 mice show an age-related deterioration in learning ability. I show here neuropathological, neurochemical and pharmacological features of SAM, especially for SAMP8 and SAMP10, and do the effects of several food materials in Hokkaido on biochemical and behavioral alterations in SAMP8, and also discuss the etiologic manifestation of accelerated senescence.

2S03: Response of mammalian cells to ionizing radiation

Kuwabara, M. (Lab. Radiat. Biol., Grad. Sch. Vet. Med., Hokkaido Univ.)

Mammalian cells undergo cell cycle while checking themselves at G1, G2 and M phases to assure the exact production of their daughter cells. The check functions are ascertained by observing the cell-cycle arrest at G1 and G2 phases followed by DNA repair in cells exposed to ionizing radiation. In the case that DNA repair is not perfect, cells positively undergo cell death called apoptosis. *p53* regulates the G1 arrest, DNA repair and apoptosis. No G1-arrest, no DNA repair and no apoptosis are induced in cells with mutated *p53*. However, it was found that human leukemia cell MOLT-4 showed apoptosis when exposed to X-rays in spite of insufficient function of *p53*, whereas human gastric adenocarcinoma MKN45 showed no apoptosis though this had a wild *p53*. These results suggest that the apoptotic induction is not necessarily dependent on *p53* status. We found that the activation of SAPK/JNK and the subsequent expression of death receptor Fas were responsible for the induction of apoptosis in MOLT-4 cells, whereas a factor associating with G2 check point played a key role in the apoptotic induction of MKN45 cells.

2S04: High power proton accelerator project and neutron science

Kiyanagi, Y. (Graduate School of Engineering, Hokkaido University)

A high power proton accelerator facility is now being constructed at JAERI as the Joint Project of JAERI and KEK. This is a multi purpose facility including a neutron-muon experimental facility (material and life science facility), a nuclear and particle physics facility, and a nuclear transmutation facility. As well known, the neutron is one of most important probes for the material and life science. So, the high intensity neutron sources based on the high power proton accelerators are under construction in the USA and planning in EU.

However, many difficulties arose which were not serious problems while the accelerator

power was not so high. As an example, we had to choose a hydrogen moderator instead of a methane moderator due to serious radiation damage. Since the neutronic performance of hydrogen is inferior to methane, we have developed a system which extremely improved the neutron intensity from the moderator. There have been many problems we solved or expect to be solved.

Here, outline of the project, usefulness of neutrons and the present status of the neutron source are presented.

1A01: Anion exchange behavior of Zr and Hf in hydrofluoric acid - Model experiments for chemical characterization of element 104, rutherfordium -

Haba, H. (Cyclotron center, RIKEN), Tsukada, K., Asai, M., Akiyama, K., Toyoshima, A., Nishinaka, I., Ichikawa, S., Nagame, Y. (Advanced Sci. Res. Center, Japan Atomic Energy Res. Inst.)

We plan to perform anion exchange experiments of rutherfordium (Rf) in HF solutions using the JAERI tandem accelerator. The distribution coefficients (K_d) on the anion exchange resin were measured in 0.17–26.1 M HF with the batch method using the carrier-free radiotracers ^{88}Zr and ^{175}Hf . It was found that the K_d values of Zr and Hf are consistent with each other and decrease steeply with an increase of HF concentration. The slope in the $\log(K_d)\text{-}\log([\text{HF}])$ plot is -3 at > 1 M indicating the formation of $[\text{MF}_7]^{3-}$ complex. We have developed the Automated Ion exchange separation apparatus coupled with the Detection system for Alpha spectroscopy (AIDA) in order to perform fast and repetitive ion exchange separations of ^{261}Rf . The model experiments for ^{261}Rf were successfully performed at 6–18 M HF using ^{85}Zr and ^{167}Hf produced in the $^{\text{nat}}\text{Ge}(^{18}\text{O},xn)$ and $^{\text{nat}}\text{Gd}(^{18}\text{O},xn)$ reactions, respectively.

1A02: Anion-exchange behavior of rutherfordium in HF media

Tsukada, K. (JAERI), Haba, H. (RIKEN), Asai, M. (JAERI), Toyoshima, A. (Osaka Univ.), Akiyama, K. (JAERI), Nishinaka, I. (JAERI), Ichikawa, S. (JAERI), Nagame, Y. (JAERI), Nakahara, H. (JAERI), Yasuda, K. (JAERI), Miyamoto, Y. (JAERI), Kaneko, T. (Niigata Univ.), Hirai, T. (Niigata Univ.), Ono, S. (Niigata Univ.), Goto, S.V, Kudo, H. (Niigata Univ.), Shigekawa, M. (Osaka Univ.), Shinohara, A. (Osaka Univ.), Sueki, K. (Tsukuba Univ.), Oura, Y. (Tokyo Metro. Univ.), Sakama, M. (Tokushima Univ.), Tsuruga, N. (Kanazawa Univ.), Kinoshita, N. (Kanazawa Univ.), Murae, T. (Kanazawa Univ.), Kikunaga, H. (Kanazawa Univ.), Yokoyama, A. (Kanazawa Univ.)

Anion-exchange behavior of Rf and Hf in 2-14 M HF media was investigated using an Automatic Ion-exchange separation apparatus coupled with the detection system for Alpha spectroscopy (AIDA). The percent adsorption of Rf on the anion-exchange resin decreases steeply with increasing HF concentration from 2.0 M to 8.0 M. It is interesting result that this adsorption behavior is quite different from that of the group-4 elements Hf and Zr.

1A03: On-line Isothermal Gas Chromatographic Behavior of Chlorides of Group IV elements as a Model Experiment of Rf (Z=104)

Kaneko, T., Tsukada, K., Akiyama, K., Asai, M., Haba, H., Toyoshima, A., Ono, S., Hirai, T., Goto, S., Ichikawa, S., Nagame, Y., Kudo, H. (Fac. of Sci., Niigata Univ., JAERI, RIKEN, Osaka Univ.)

The behavior of Zr and Hf in the gas system Cl_2/CCl_4 on SiO_2 surface was investigated using the methods of online isothermal gas chromatography. The adsorption data of hafnium and zirconium chloride with the temperature of $50^\circ\text{C} - 400^\circ\text{C}$ were evaluated. It was found that Zr and Hf chlorides behaved similarly in this system. Therefore, the adsorption behavior of chlorides of these elements for quartz surface is not differing each other. That is reasonable

for expectation from sublimation enthalpy in macro scale.

1A04: Study of cation exchange behavior of nobelium(III)

TOYOSHIMA, A. (Osaka Univ.), TSUKADA, K. (JAERI), SHIGEKAWA, M. (Osaka Univ.), HABA, H. (RIKEN), ASAI, M. (JAERI), AKIYAMA, K. (JAERI), NISHINAKA, I. (JAERI), TANI, Y. (Osaka Univ.), HASEGAWA, H. (Osaka Univ.), ICHIKAWA, S. (JAERI), NAGAME, Y. (JAERI), KANEKO, T. (Niigata Univ.), HIRAI, K. (Niigata Univ.), SHINOHARA, A. (Osaka Univ.)

It is important to investigate the ionic radius of nobelium(III) in order to clarify the irregularity of that of lawrencium(III) compared to heavy lanthanides. Thus, we have a plan to perform a cation exchange experiment of No(III) under an oxidation condition. In this study, we investigated a cation exchange behavior of heavy lanthanide with the rapid ion exchange apparatus as a basic data on No(III).

It was shown the relationship between the distribution coefficients for Er, Ho, Dy and Tb and the ionic radii of 6 coordinate. Thus, we can obtain the ionic radius of No(III) with this relationship because the distribution coefficient for nobelium is expected between Er and Ho.

1A05: Ionization and on-line mass-separation of berkelium and nobelium isotopes

Asai, M., Tsukada, K., Ichikawa, S., Nagame, Y., Nishinaka, I., Akiyama, K., Toyoshima, A., Osa, A., Haba, H., Sakama, M., Oura, Y., Kojima, Y., Shibata, M., Sueki, K. (Advanced Sci. Res. Center, JAERI; Radioisotope Technol. Div., RIKEN; Dep. Radiologic Sci. and Engineering, Univ. Tokushima; Dep. Chemistry, Tokyo Metropolitan Univ.; Graduate School of Engineering, Hiroshima Univ.; Facility for Nucl. Materials, Nagoya Univ; Dep. Chemistry, Tsukuba Univ.)

Efficiencies of on-line mass separation for berkelium and nobelium isotopes have been measured using the JAERI on-line isotope separator. Ionization efficiencies for Bk-250 and No-257 were determined to be 2.2% and 0.9%, respectively, which are high enough to perform nuclear decay spectroscopy.

1A06: JAERI-KREK joint RNB project

ICHIKAWA, S. (JAERI)

Japan Atomic Energy Research Institute (JAERI) and High Energy Accelerator Research Organization (KEK) are jointly constructing an ISOL-based medium size radioactive nuclear beam (RNB) facility at the JAERI tandem accelerator. This facility consists of the Tandem accelerator, JAERI-ISOL, a charge-breeding electron cyclotron resonance ion-source (CB-ECRIS), a split-coaxial RFQ (SCRFAQ) linac, an interdigital-H (IH-) linac, a pre-booster linac and a superconducting (SC-) linac, in which the pre-booster linac and CB-ECRIS will be newly constructed. The CB-ECRIS will breed charge states of ions from ISOL to inject them into the post linaces that require low mass-to charge (A/q -) ratios for acceleration. The heavy neutron-rich RNB produced by fission as well as light RNB will be available from FY 2004 with energy up to 1.09 MeV/u. The pre-booster linac will be built in future for injecting RNB into the existing SC-linac to increase the beam energy beyond the Coulomb barrier for all kinds of targets.

1A07: Development of Ion Sources for JAERI-ISOL in JAERI-KEK Joint RNB Project

OSA, A., MATSUDA, M. (Dept. Materials Sci., JAERI), ICHIKAWA, S., TSUKADA, K., ASAI, M. (Adv. Sci. Res. Center, JAERI), JEONG, S. C., KATAYAMA, I. (KEK)

An ISOL-based radioactive nuclear beam (RNB) facility is under construction to provide RNBs having energy up to 1 MeV/u. We are developing a cavity type thermal ion source and FEBIAD type ion source for JAERI-ISOL. Release time and overall efficiency of several

elements from the target-catcher-ion-source system were measured using the heavy ion implantation technique. In this method, the stable isotopes accelerated by the tandem accelerator were implanted into the target/catcher inside the ion source. Time dependence of the mass-separated beam intensity after switching off the primary beam corresponds to the release behavior. Also, the ratio of primary and mass-separated beam is given as the separation yield.

The RNB, ^8Li , ^{18}F and ^{20}F nuclei, will be used to study thermal diffusion processes in materials at the very early stage of the RNB facility. We have investigated the release time of Li atom and separation yield of ^8Li , and molecular-ion formation of F atom to produce the RNBs of ^8Li , ^{18}F and ^{20}F .

1A08: Measurement of production cross sections for 12 GeV proton reaction with Hg target used as spallation neutron source

Numajiri, M., Miura, T., Suzuki, T. (Radiation Sci. Center, High Energy Accelerator Res. Organization), Kondo, K. (Applied Res. Lab., High Energy Accelerator Res. Organization)

Irradiation experiments were performed in order to investigate the production cross-sections of residual nuclei by proton induced reactions at KEK proton synchrotron facility. Production cross-sections in a Hg target, which will be used as spallation neutron sources, were measured by gamma-ray spectroscopy. The present data are compared with the previous results for other heavy elements.

1A09: Q_β determination of fission products with a total absorption detector without decay scheme

Ichikawa, S. (JAERI), Shibata, M., Suematu, O. (Nagoya Univ), Kojima, Y. (Hiroshima Univ.), Taniguchi, A. (Kyoto Univ.), Asi, M., Tsukada, K., Osa, A., Akiyama, K., Nagame, Y. (JAERI),

For Q_β determination of rare nuclei like new isotopes with accuracy of 0.3 MeV, we have developed a total absorption detector. This detector consists of two identical large volume ($12\text{ cm}^\phi \times 10\text{ cm}$) and low background (^{207}Bi free) BGO scintillators that are put in face to face with distance 3 mm. Efficiencies for monoenergetic electrons and photons at 8 MeV were evaluated to be 90% and 75% full energy peak, respectively. Owing to its high efficiency, all β -ray end-points concentrate the same position in energy spectrum since β -rays that decay to excited states are completely summed up with successive γ -rays. Then the end-point of energy spectrum is equal to Q_β . This detector was installed at JAERI-ISOL in order to determine Q_β of the previously identified new isotopes produced in the proton-induced fission of ^{238}U . So far, Q_β values of ^{158}Pm , ^{159}Pm , ^{159}Sm and ^{166}Tb were determined. Observed values are in good agreement with the evaluated values by Audi *et al.*

1A10: Alpha-decay from the nuclear isomer of Th-229 with extremely low excitation energy

Kikunaga, H., Kinoshita, N., Yokoyama, A.¹, Nakanishi, T.¹, Mitsugashira, T.², Hara, M.², Ohtsuki, T.³, Yuuki, H.³, Takamiya, K.⁴, Kasamatsu, Y.⁵, Shinohara, A.⁵ (Graduate School of Natural Sci. and Technol., Kanazawa Univ., Fac. of Sci., Kanazawa Univ.¹, Oarai-branch, IMR, Tohoku Univ.², Lab. Nucl. Sci., Graduate School of Sci., Tohoku Univ.³, Res. Reactor Inst., Kyoto Univ.⁴, Graduate School of Sci., Osaka Univ.⁵)

We attempted to observe the alpha-particles from $^{229\text{m}}\text{Th}$ which is a nuclear isomer with extremely low excitation energy. The $^{229\text{m}}\text{Th}$ atoms were produced with ^{230}Th (photon, n) $^{229\text{m}}\text{Th}$ and ^{232}Th (photon, p2n) ^{229}Ac --beta--> $^{229\text{m}}\text{Th}$ reactions, in this study. The bremsstrahlung irradiation was carried out using electrons of 27 MeV from the linear accelerator of Tohoku University. After the irradiation, Th and Ac were isolated from the targets to prepare sources for alpha-spectrometry. We observed some alpha events attributable

to ^{229m}Th in the expected energy region of the spectra. The data is, however, still in the process of analysis.

1A11: Production and decay property of ^{229m}Th using $^{228}\text{Ra}(n, \gamma)^{229}\text{Ra}$ reaction

Kasamatsu, Y.¹, Kimura, H.¹, Takamiya, K.², Ninomiya, K.¹, Yatsukawa, M.¹, Shibata, S.², Yamana, H.², Ohkubo, Y.², Mitsugashira, T.³, Shinohara, A.¹ (1 Graduate School of Sci. Osaka Univ., 2 Research Reactor Institute, Kyoto Univ., 3 The Oarai-branch, Institute for Materials Research, Tohoku Univ.)

The existence of a low energy isomeric state of ^{229}Th has been reported. The nucleus is expected to decay mainly via an electron bridge mechanism because of its extremely low excitation energy. We tried to produce ^{229m}Th using the following nuclear reaction; $^{228}\text{Ra}(n, \gamma)^{229}\text{Ra}$. ^{229}Ra decays into ^{229}Ac and ^{229}Ac decays into ^{229}Th . After irradiation, Ac was separated from Ra and Th by solvent extraction using HDEHP (bis(2-ethylhexyl)phosphoric acid). The half of the separated sample was coprecipitated with samarium as a source for alpha-ray detection. The other was left for about 3 hours to wait until most of ^{229}Ac decayed into ^{229}Th . Then, grown Th was isolated by anion exchange method and assayed to photon measurement with a photomultiplier.

1A12: Measurement of excitation function of $^{63}\text{Cu}(n, p)^{63}\text{Ni}$ at $E_n < 6.5\text{MeV}$

Ohta, Y.¹, Takamiya, K.², Shibata, S.², Shibata, T.³, Itoh, Y.³, Imamura, M.⁴, Uwamino, Y.⁵, Nogawa, N.⁶, Baba, M.⁷, Iwasaki, S.⁷, Matsuyama, S.⁷ (Grad. School of Eng., Kyoto Univ.¹, Res. Reactor Inst., Kyoto Univ.², Radiation Sci. Center, High Energy Accelerator Res. Org.³, Nat. Mus. of Japanese Hist.⁴, RIKEN⁵, RI Centre, Univ. of Tokyo⁶, Grad. School of Eng., Tohoku Univ.⁷)

The excitation function of $^{63}\text{Cu}(n, p)^{63}\text{Ni}$ has been measured at neutron energies below 6.5 MeV. This excitation function is indispensable to estimate radioactivity of ^{63}Ni produced in copper materials at reactor and accelerator facilities and can also be applied to estimate a neutron fluence of the Hiroshima and Nagasaki atomic bombs. However, cross section data at neutron energy range below 10 MeV is rather scanty. Therefore, relevant excitation function measurement in this energy range is required. The irradiation of samples with 1.7~6.4 MeV neutrons was carried out at FNL in Tohoku University. The ^{63}Ni and ^{60}Co produced in the copper samples were chemically separated and measured by low background liquid scintillation counter and Ge detector, respectively. The results of measurements for several samples were previously presented. In this presentation, the results of all samples in whole energy region of 1.7~6.4 MeV will be shown.

1A13: Yield measurements of photospallation products at intermediate energies by radiochemical technique

MATSUMURA, H. (Radiation Sci. Center, KEK), AZE, T. (Graduate School of Integrated Basic Sci., Nihon Univ.), OURA, Y. (Graduate School of Sci., Tokyo Metropolitan Univ.), KIKUNAGA, H. (Graduate School of Natural Sci. and Technol., Kanazawa Univ.), YOKOYAMA, A. (Fac. of Sci., Kanazawa Univ.), TAKAMIYA, K., SHIBATA, S. (Res. Reactor Inst., Kyoto Univ.), OTSUKI, T., YUKI, H. (Lab. of Nucl. Sci., Tohoku Univ.), SAKAMOTO, K. (Fac. of Sci., Kanazawa Univ.), HABA, H. (Cyclotron Center, RIKEN), WASHIYAMA, K. (Fac. of Medicine, Kanazawa Univ.), NAGAI, H. (Coll. of Humanities and Sci., Nihon Univ.), MATSUZAKI, H. (Res. Center for Nucl. Sci. and Technol., The Univ. of Tokyo)

In this study the measured yields of photospallation from ^{197}Au target in irradiation with bremsstrahlung having maximum end-point energies, $E_0=200\text{MeV}$ were added to our many accumulated ones from other targets. The yields were applied to empirical formula of Rudstam which had five unknown parameter, and the charge distributions and the mass yields

were obtained. The experimental data were also compared with the results from the PICA3/GEM codes. We will discuss on photospallation with the information from the comprehensive survey.

1A14: RNAA coupled with the k_0 -method - An attempt of determining trace halogens in rock samples -

Ozaki, H., Ebihara, M. (Res. Center Nucl. Sci. Tech., Univ. of Tokyo, Graduate School Sci., Tokyo Metropolitan Univ.)

The k_0 -standardization neutron activation analysis (k_0 -method) requires no comparative standards for determining elemental concentrations of samples. So far, the k_0 -method has been used for INAA, where many elements can be determined simultaneously with no chemical standards. In this study, the k_0 -method was utilized for radiochemical neutron activation analysis (RNAA) for halogens in rock samples. This must be effective especially for iodine, because the preparation of iodine chemical standard and its handling involve several potential factors causing analytical errors. Analytical results obtained by the k_0 -method agree with reference values and also with results obtained by comparative method.

1A15: Element analysis of medaka by instrumental neutron activation analysis with the k_0 -standardization method

Mastushita, R., (Grad. Sch. Sci. Tech., Kumamoto Univ.), MOMOSHIMA, N. (Fac. Sc. Kumamoto Univ.)

The aim of this work was multielement analysis of medaka (*Oryzias latipes*) and gambusia (*Gambusia affinis*) by k_0 -standardization method of instrumental neutron activation analysis (k_0 -INAA). The samples of medaka and gambusia were collected in Midori River, Kikuchi River and Shira River located on Kumamoto in Japan. We collected these samples every month at there. The samples were irradiated by JRR-4 at Toukai Institute of Japan Atomic Energy Research Institute (JAERI). Samples were irradiated 1 hour, 2 hours and 5 hours on condition that output of reactor is 100kW and thermal neutron flux is 1.51×10^{12} n/cm²s. Each sample was measured three times by Twin Detector-Auto Sample Changer (TD-ASC) for determination of element concentrations. In result, we determined 6 elements (Na, K, Mn, Zn, Br, Sr). The element concentrations did not show a correlation with sample weight, sampling locating and month.

1A16: Determination of As, I, and Br in edible seaweeds by neutron activation analysis

FUKUSHIMA, M. (Ishinomaki Senshu Univ.) ISAAC-OLIVE, K., CHATT, A. (Dalhousie Univ.)

Iodine is one of essential elements for human diets, and it is well known that seaweeds are excellent sources of Iodine. Concentrations of Iodine and Bromine in Japanese edible seaweeds were obtained by epi-thermal instrumental neutron activation analysis, and also Arsenic by neutron activation analysis in SLOWPOKE-2 Facility, Dalhousie University, Canada. Samples were; raw glue plant (funori), raw and baked laver (nori), raw sea lettuce, dried hizikia (hijiki), dried Japanese tangle (konbu), raw sea mustard (wakame), raw and baked fir needle (matsumo). In order to estimate the bioavailable iodine, seaweeds were digested by enzymolysis, the residue of digestion and water-soluble dietary fiber (WSDF) were dried and irradiated, and the iodine levels were obtained. We estimated the levels of bioavailable iodine by suppressing the iodine in WSDF from total iodine. The concentrations of Iodine, Bromine, Arsenic, and the ratio of bioavailable iodine to total iodine in seaweeds differed much between the species of seaweeds.

1A17: Determination of Arsenic in Groundwater and Foodstuffs using Instrumental Neutron Activation Analysis (INAA)

(INST, Bangladesh Atomic Energy Commission,¹ Dept. of Physics, SUST, Bangladesh,² Graduate School of Sci., Tokyo Metropolitan Univ.³) ○Sk. A. Latif¹, M. A. Halim¹, M. N. Chowdhury¹, K. Naher¹, M. A. Hafiz¹, R. U. Miah¹, F. U. Ahmed¹, M. A. Islam,² M. I. Hossain,² and M. Katada³

In Bangladesh, tube-wells water of most of the districts is polluted by As. Recently, it is reported that vegetables and crops are also highly contaminated by As. To assess the potential sources of As, a parallel study of groundwater, surface water, soils and foodstuffs collected from different districts were conducted using Instrumental Neutron Activation Analysis. The samples and standards were simultaneously irradiated at 250 kW for 2.5 hours using 3 MW TRIGA Mark-II Research Reactor, Dhaka. The detection limit of As determined under the present experimental conditions was 7.8 ± 0.6 ng/g. The standard reference material 1643d was used to evaluate this method. The results are in good agreement ($\pm 10\%$) with the certified values. Groundwater samples collected from northwestern part of Bangladesh were highly contaminated (21-2761 $\mu\text{g/L}$). Whereas the surface water was free from arsenic contamination. Arsenic was detected only in two foodstuffs (Arum) of Comilla district.

1A18: Effects of slight zinc deficiency on concentrations of trace elements in organs and tissues of mice

Ogi, T., Kawamoto, Y., Maetsu, H., Koike, M., Ohyama, T., Noguchi, M., Suganuma, H., Yanaga, M. (Fac. of Sci., Shizuoka Univ.)

Effects of slight zinc deficiency on concentrations of trace elements in various organs and tissues of mice were investigated. Eight-week old male mice of ICR strain were divided into four groups, and fed with diet containing different concentration of zinc, <1, 3, 7, and 30 $\mu\text{g/g}$, respectively, for one or three weeks. Concentrations of twelve elements in liver, kidney, pancreas, testis, and bone were determined by instrumental neutron activation analysis. Zinc concentration in plasma was also determined by PIXE analytical technique. Zinc concentrations in bone and pancreas were decreased with a decrease of zinc content in diets. Contrary to the zinc concentration, cobalt concentrations were increased in the reverse order. It is concluded that not only serious but slight zinc deficiency effects on the metabolism of trace elements in organs and tissues, although no apparent symptoms due to zinc deficiency were recognized.

1A19: Subcellular distribution of trace elements in livers of Zn-deficient mice

Ohyama, T., Koike, M., Ogi, T., Kawamoto, Y., Maetsu, H., Suganuma, H., Noguchi, M., Ishikawa, K., Hirunuma, R., Enomoto, S., Yanaga, M. (Graduate School of Science and Engineering, Shizuoka University and RIKEN)

In order to investigate the influence of Zn deficiency on biobehaviour of trace elements, concentrations of essential trace elements in subcellular fractions of livers of Zn-deficient mice were determined. Three or eight-week old male mice of ICR strain were divided into two groups. One group was fed with Zn-deficient diet and distilled water, and the other group was fed with control diet and the same water. After three weeks, their livers were removed and weighed immediately. These livers were divided into four subcellular fractions, such as nuclear, mitochondrial, microsomal and supernatant fraction by ultracentrifugation. In this study, the concentrations of ten trace elements (Na, Mg, Cl, Mn, Fe, Co, Cu, Zn, Se and Rb) were determined by INAA. In both 3 and 8-week old mice, Zn concentration in nuclear fraction of Zn-deficient mice was higher than that of control ones. About the concentration of Fe, an increase in concentration was recognized in microsomal fraction of 3-week old mice alone.

1A20: Radiochemical activation analysis of trace Mo and W in geochemical and

cosmochemical samples

Motohashi, T.¹, Sueki, K.², Oura, Y.¹, Ebihara, M.¹ (Graduate School of Sci., Tokyo Metropolitan Univ.¹, Dep. of chemistry, Univ. of Tsukuba²)

Using radioactive tracers, chemical procedure for separating Mo and W from geochemical and cosmochemical samples was developed in order to determine these elements by radiochemical neutron activation analysis (RNAA). Mo and W in 10M HF were adsorbed on anion exchange resin, which was then washed by 12M HCl, and Mo and W were eluted by 3.5M HNO₃ + 5% H₂O₂. This procedure was applied to some geochemical standard rock samples. W data were consistent with their literature values, but those of Mo were generally higher. This must be caused by the contribution of ²³⁵U(n, f) reaction. An experimental approach for estimating the contribution of fission products is in progress.

1A21: Determination of trace thorium and uranium in geochemical and cosmochemical samples by ICP-MS: Comparative study with RNAA

Chai, J.Y.^{1,2}, Miyamoto, Y.², Saito, Y.², Oura, Y.¹, Ebihara, M.¹, Magara, M.², Sakurai, S.², Usuda, S.²(Graduate School of Sci., Tokyo Metropolitan Univ.¹, JAERI²)

We aim to develop a practical chemical procedure of inductively coupled plasma mass spectrometry (ICP-MS) for elemental and isotopic determination of trace Th and U in terrestrial and extraterrestrial rock samples with high accuracy and precision. After being purified by anion-exchange, Th and U were determined by ICP-MS. The analytical procedure was applied to several geological rock reference standards prepared by Geological Survey of Japan (GSJ). Analytical results thus obtained were compared with the recommended values of GSJ and our radiochemical neutron activation analysis (RNAA) data. We found that all our ICP-MS data agree well (within 10%) with the recommended values and our RNAA data, suggesting that Th and U are quantitatively recovered in their purification step. Relative standard deviations were around 5% (1σ) for Th and U in 5 parallel analyses.

1A22: Application of high sensitive determination by using multiparameter coincidence method-Analysis for an ancient Chinese bronze vessel-

Hatsukawa, Y., Shinohara, N., Toh, Y., Oshima, M.(Japan Atomic Energy Research Institute)

The method of multiparameter coincidence spectrometry based on γ-γ coincidence is applied to determination of trace elements in an ancient Chinese bronze vessel. The bronze vessel was produced in Shang dynasty (1500-1050 BCE). The powdered sample (41.208 mg) collected from the bronze vessel was irradiated at a JAERI's research reactor for 5 sec, 15 min., and 8 hours. Irradiated sample was placed at center of a multiparameter coincidence spectrometer, GEMINI, and measured multiple γ rays from the isotopes produced by neutron capture reactions. 29 elements in the bronze vessel, Ca, Sc, Ti, Fe, Mn, Co, Cu, As, Se, Br, Mo, Ag, Cd, Sb, Sn, Cs, Ba, La, Ce, Gd, Tb, Yb, Lu, Hf, Ta, Ir, Au, Th, and U were determined.

1B01: A formation process and characterization of technetium(IV) oxide colloids by bremsstrahlung irradiation of an aqueous solution of pertechnetate

Sekine, T., Narushima, H., Kudo, H., Suzuki, T.(Graduate School of Science, Tohoku Univ.), Lin, M., Katsumura, Y. (School of Engineering, Univ. Tokyo)

We have found formation of technetium(IV) oxide colloids by bremsstrahlung irradiation of an aqueous pertechnetate solution saturated with Ar gas. The mean size of colloid particles distributed in the range from 15 to 80 nm. The particles were aggregates of a number of tiny particles around 2 nm in diameter. The yield of the colloids increased with an increase of absorbed dose at pH beyond 3, while no colloids formation was observed in acidic solutions. This fact suggests a significant contribution of hydrated electrons (a radiolysis product of

water) on the reduction process of pertechnetate ions, because hydrated electrons are effectively eliminated in acidic solutions through the reaction with protons.

1B02:Crystal structure of technetium(IV) complex [TcCl₂(dmsalen)] with salen type Schiff base ligand

Takayama, T., Sekine, T., Kudo, H. (Graduate School of Sci. Tohoku Univ.)

The novel technetium(IV) complex of tetradentate Schiff base ligands was synthesized from the reaction with [TcNCl₂(PPh₃)₂] and H₂dmsalen. The complex was characterized by IR spectroscopy and X-ray crystallography. The IR spectrum shows the absorption of C=N stretch frequency at 1610 cm⁻¹. And the absorption of C-O stretch frequency appears at 1288 cm⁻¹. X-ray structure determination shows that the technetium(IV) complex of tetradentate Schiff base ligands [TcCl₂(dmsalen)] has octahedral coordination geometry. The technetium atom was coordinated with the two N and two O donor atoms of tetradentate Schiff base ligand in the equatorial plane and the two chloro ligands in the trans apical position.

1B03:Synthesis of novel nitridotechnetium(V) complexes of salen type Schiff base ligands with benzyl group

ABE, Y., TAKAYAMA, T., SEKINE, T., KUDO, H. (Graduate School of Sci., Tohoku Univ.)

Two salen type Schiff base ligands monosubstituted in the bridging alkyl group, 2,2'-(2-R-1,3-propanediylbis(nitrilomethylidene)bis(phenolato)) (R=benzyl, *p*-nitrobenzyl) were synthesized. The structures of both ligands were characterized by ¹H NMR spectroscopy. Nitridotechnetium complexes of these ligands were prepared by ligand exchange reaction of [TcNCl₂(PPh₃)₂] with the corresponding salen type Schiff base ligands in CH₂Cl₂. The results of TLC analysis for the reaction mixture showed that the product consisted of two similar species in the 2:3 ratio. The ¹H NMR spectrum was obtained for the mixture of these two species. The spectrum indicated that two imido protons in the complexes were in the same environment. Two sets of ¹H NMR resonances were observed for the methylene protons of the benzyl group. Integration of the two ¹H NMR resonances showed that the ratio of the two species was approximately 2:3, indicating the existence of *anti* and *syn* isomers with respect to the technetium nitrido and benzyl groups.

1B04:Synthesis of nitridotechnetium(V) complexes of propylene amine oxime (PnAO) with benzyl group •Production of *syn* and *anti* isomers•

MORIMOTO, Y., TAKAYAMA, T., SEKINE, T., KUDO, H. (Graduate School of Sci., Tohoku Univ.)

Three propylene amine oxime (PnAO) ligands monosubstituted in the 6-position, 3,3,9,-tetramethyl-6-R-4,8-diazaundecane-2,10-dionedioxime (R=benzyl, *p*-nitrobenzyl and *p*-aminobenzil) were synthesized. Nitridotechnetium complexes of these ligands were prepared by ligand exchange reaction of [TcNCl₂(PPh₃)₂] with corresponding PnAO ligand. The results of ¹H NMR showed that two main species were produced and that the ratios of each pair of products were about 1 : 1. The pairs of the complexes were assigned to be *syn* and *anti* isomers of the complex cation [TcN(PnAO-6-R)]⁺. The X-ray crystallographic results for both *syn* and *anti* isomers of the complexes [TcN(PnAO-6-benzyl)(H₂O)][PF₆]⁻ were similar to that obtained for other complexes with the [TcN(PnAO)]⁺ cation. The coordination around technetium atom was the distorted octahedral; the four N atoms of the PnAO ligand were in the equatorial plane and the nitrido and H₂O ligands at the axial positions.

1B05:Mobile phase of supercritical fluid chromatography for lithium isotope separation

Watanabe, T. (Department of Nuclear Engineering, Nagoya University), Tomioka, O. (Research Center for Nuclear Materials Recycle, Nagoya University), Enokida, Y. (Research Center for Nuclear Materials Recycle, Nagoya University), Yamamoto, I. (Department of Nuclear Engineering, Nagoya University)

Chromatographic lithium isotope separation was performed in a break through manner. Cryptand (2_B,2,1) resin and a mixed fluid of supercritical CO₂ and LiCl in methanol were used for stationary phase and mobile phase, respectively. It is considered that the molar fraction of CO₂ in mobile phase affects the total capacity of cryptand (2_B,2,1) and the enrichment factor of lithium isotope. The experiments were done at 313 K, 10 MPa. The molar fraction of CO₂ in mobile phase was varied between 0 and 0.47. It was found that the total capacity was varying, and the enrichment factor was decreasing with increasing molar fraction of CO₂. This means that the behavior of adsorption of LiCl and cryptand (2_B,2,1) was changed since the salvation of mobile phase was changed.

1B06:Variable temperature Mössbauer spectroscopic studies of new oxo-centered trinuclear mixed valence iron dicarboxylic acid complexes.

D. Afroj, M. Katada. (Graduate School of Science, Tokyo Metropolitan University)

Two new oxo-centered trinuclear mixed valence iron dicarboxylic acid complexes, iron isophthalate and iron mesaconate have been prepared. Variable temperature Mössbauer spectroscopic studies suggest temperature dependent valence delocalization processes for both the complex. At liquid nitrogen temperature the spectra consist of two quadrupole split doublets correspond to high spin Fe(III) and Fe(II) state for both complexes. The area ratios of the two doublets were very close to the theoretical value (2:1) of oxo-centered trinuclear mixed valence iron complexes. With increasing temperature the rate of intramolecular electron transfer also increases and the two doublets move together to become a single doublet. The room temperature spectra showed asymmetric doublets for both complexes showing the parameters consistent with the average valence state of high spin Fe(III) and Fe(II). The asymmetries of the doublets indicate the presence of small amount of Fe(III) as an impurity in both complexes. DSC measurements showed no phase transition and TG-DTA measurements indicated the presence of solvated water molecules in the complexes.

1B07:Synthesis and characterization of the borate-vanadate glasses(2)

Tachibana, H.,Katada,M.(Graduate School of Science,Tokyo Metropolitan Univ.)

In a series of $xR_2O \cdot (1-x)(B_2O_3-V_2O_5)$ glasses ($x = Li, Na, K$), we found that alkali-rich glasses were prepared, the values of their isomer shifts (IS) were affected by vanadium atom, and the dependence of quadrupole splitting (QS) on the content of the alkali metal was reverse those found in ordinary alkali glasses. In this study, we made new glasses by adding germanium oxide as the glasses former in stead of borate oxide, and investigated the local structural differences between borate-vanadate and germanate-vanadate glasses. We prepared also the three-component-glasses of borate-germanate-vanadate to find new physico-chemical properties for these glasses.

1B08:Photo-induced spin transition of ferrocene in PMMA matrix.

Einaga, Y., Kotake, M., Akitsu, T. (Keio Univ.), Yamada, Y. (Tokyo Univ. of Science), Sato, O. (KAST)

There has been a great interest in developing novel molecular compounds whose spin states can be controlled by photo-illumination. Here, we will present a matrix isolation technique as a potentially new strategy for realizing such a system. Poly(methyl methacrylate) (PMMA) matrices films containing ferrocene were prepared by casting mixed acetone solution of polymer, Cp₂Fe and CCl₄ on a clean glass plate at room temperature. High spin isomeric Cp₂Fe were produced by UV-illumination of Cp₂Fe isolated in the matrices. ⁵⁷Fe Mössbauer spectra showed that high spin Cp₂Fe was produced as well as ferricinium ion [Cp₂Fe]⁺ on the illumination. The photo-induced spin transition of Cp₂Fe in PMMA matrices were also confirmed by means of SQUID

measurements. The matrix isolation technique for detecting the unstable species can be used as a novel strategy for preparation of optically switchable molecular solids.

1B09: Mössbauer spectroscopic study of spin-crossover Fe(II)-Fe(III) complexes

Iijima, S., Mizutani F. (Natl. Inst. Adv. Ind. Sci. Technol.), Ikuta, Y., Oidemizu, M., Matsumoto, N. (Fac. Sci., Kumamoto Univ.), Sunatsuki, Y., Ohta, H., Kojima, M. (Fac. Sci., Okayama Univ.)

Mixed-valence spin-crossover complexes $[\text{Fe}^{\text{II}}\text{H}_3\text{L}][\text{FeL}]\text{X}_2$ ($\text{X}^- = \text{BF}_4^-$ and NO_3^-) were investigated by ^{57}Fe Mössbauer spectroscopy, where $\text{H}_3\text{L} = \text{tris}[2-\text{((imidazol-4-yl)methylidene)amino}]\text{ethylamine}$. The Mössbauer spectrum at 78 K of each compound consisted of double doublets showing low-spin Fe^{II} and low-spin Fe^{III} states. On elevating the temperature over 150 K, the Fe^{II} site of $\text{X}^- = \text{BF}_4^-$ salt began to show spin-crossover behavior, and fully turned to the high-spin state around at 250 K. An absorption of Fe^{III} high-spin state indicating the spin-crossover of the Fe^{III} site appeared over room temperature. A similar successive spin transition of Fe^{II} and Fe^{III} sites were observed for $\text{X}^- = \text{NO}_3^-$ salt. In the latter compound, the high-spin/low-spin ratio of Fe^{II} site depended on the cooling-down process.

1B10: Construction and optical property for photo-induced spin transition compound

Hayami, S., Kawahara, T., Maeda, Y. (Kyushu Univ.)

Recently, we have found that an iron(III) compound, $[\text{Fe}(\text{pap})_2]\text{ClO}_4$ with tridentate planar ligands shows an abrupt spin transition with hysteresis loop and light-induced excited spin state trapping (LIESST) effects below 100 K by illuminating green light. Here, we show that an iron(III) compound, $[\text{Fe}(\text{qsal})_2]\text{NCS}$ (**1**), with tridentate planar ligands exhibits LIESST effect below 40 K by irradiation at 800 nm. In fact, an increase in the magnetization was observed, when the ligand-to-metal charge transfer band of the sample was excited at 5 K in a SQUID cavity with a semiconductor laser. This shows that the LIESST effect was induced by illumination. The change persisted for periods of at least ten hours at 5 K, and the total relaxation from high-spin to low-spin was induced above 40 K. That is, **1** has a bistable nature below 40 K. This is the second example of iron (III) complexes, of which show the LIESST effect. We will discuss about the LIESST effect for **1** by using Mössbauer spectroscopy.

1B11: Synthesis and properties of LIESST iron (II) polynuclear compounds

KAWAMURA, K., HAYAMI, S., INOUE, K., MAEDA, Y. (Kyushu University, Institute for Molecular Science)

A number of spin-crossover iron(II), iron(III) and cobalt(II) compounds have been studied. Some of the iron(II) compounds exhibit spin transition from low-spin (LS, $S = 0$) to metastable high-spin (HS, $S = 2$) states by illumination at low temperature. The Light-Induced Excited Spin-State Trapping (LIESST) effect has often investigated on mononuclear compounds. There are only a few LIESST iron (II) polynuclear compounds. Here we have attempted to prepare polynuclear iron (II) LIESST compounds. $[\text{Fe}(\text{bpn})(\text{NCS})_2]$ (**1**) and $[\text{Fe}(\text{bpe})(\text{NCS})_2]$ (**2**) were synthesized. Where **bpn** is a abbreviation of *N,N'*-bis(2-pyridylmethylidene)-1,5-diiminonaphthalene and **bpe** is a abbreviation of *N,N'*-bis(2-pyridylmethylidene)-1,2-diiminoethane. The magnetic properties of the compounds were examined by magnetic susceptibility and Mössbauer spectroscopy.

1B12: Metal-dilution studies on an iron(III) spin-crossover compound with relaxation

(九大院理, KAST) Juhász Gergely, Shinya Hayami, Osamu Sato, Yonezo Maeda

The spin-crossover compound $[\text{Fe}(\text{qsal})_2]\text{NCS}$ (**1**) was investigated by Mössbauer

spectroscopy. At low temperatures a doublet with typical IS and QS parameters of iron(III) LS state was observed, however at room temperature the component for the HS state has a broad spectrum. Although the HS \leftrightarrow LS relaxation is generally fast in the case of iron(III) coordination complexes between the HS and LS states, the hysteresis loop shows that the both the LS and HS states are bistable from around 200 K to 300 K in compound 1. The line-broadening is also observed in the spectra of pure HS compound [Fe(qsal)₂]Cl (2). In order to investigate the role of intermolecular interactions on the observed relaxation, the Mössbauer spectra for aluminum diluted compounds (i.e. a part of the iron(III) content of the sample was exchanged to aluminum(III)) were also measured and evaluated.

1B13: Study on arene complex of tetraphenylene

Nakashima, S., Nishikawa, T.¹, Okuda, T.¹ (Radioisotope Center, Hiroshima Univ., Graduate School of Sci., Hiroshima Univ.¹)

FeCp⁺ and FeCp²⁺ complexes of tetraphenylene were synthesized. Mass spectrum showed the existence of mononuclear complex. Tetraphenylene has saddle structure, having 4-fold rotatory inversion axis; i. e., there are four equivalent benzene rings. Nevertheless, polynuclear complexes were not obtained. ⁵⁷Fe Moessbauer spectra showed ferrocene-like Fe^{II} doublet. The Q.S. value of FeCp²⁺ complex is smaller than that of FeCp⁺ complex. The decrease in Q.S. value is explained by the increase in the back donation of d_{x²-y²} and d_{xy} electrons from iron to tetraphenylene by introducing methyl substituents to Cp ring.

1B14: ¹²¹Sb Mössbauer spectra for some zirconium antimonide

Kitadai, K.; Takahashi, M.; Takeda, M. (Department of Chemistry, Faculty of Science, Toho Univ.)

In the zirconium antimonides, antimony atoms adopt various structures; for example planar zig-zag chains, linear chains or two dimensional sheet structures. This work was carried out to obtain the information on the electronic states of the antimony atoms in zirconium antimonides using ¹²¹Sb Mössbauer spectroscopy. Samples were prepared by reacting stoichiometric amounts of zirconium and antimony in an evacuated quartz tube at 950 °C. The products were identified by XRD. ¹²¹Sb Mössbauer spectra were measured at 12 K. The value of isomer shift (δ), relative to InSb, indicates that the electronic state of antimony atoms in Zr₅Sb₃ is isoelectronic to those in M₃Sb (M = Na, K). Two antimony sites ($\delta = -1.73$ and -0.21 mm s⁻¹) are observed in ZrSb₂, in good agreement with the result of X-ray determination. Although the crystal structure of Zr₂Sb₃ is unknown, the Mössbauer spectrum suggests that there are two kinds of antimony sites, one is Sb⁻ like and may have chain-like structure, and the other is Sb³⁻ like and may be isolated anions.

1B15: Monitoring of the atmospheric environment using the state analysis of corroded iron plates by Moessbauer spectroscopy

Ikeda, K., Kuno, A., Matsuo, M. (Graduate School of Arts and Sci., The Univ. of Tokyo)

Iron plates exposed to the ambient atmosphere at several locations in Tokyo metropolitan area for two weeks were analyzed by the conversion electron Moessbauer spectroscopy (CEMS) in an attempt to monitor the atmospheric environment. Each spectrum of sample plates collected had a sextet (Fe) corresponding to metallic iron and a doublet (Fe(III)) which was due to the corrosion products formed on the plate. The correlation between the value of Fe(III)/Fe and the concentration of NO₂ (mainly due to car exhaust) at most monitoring locations was recognized. This indicates that the car exhaust affects the corrosion of iron. However, at some locations, the values of Fe(III)/Fe are not high in spite of high traffic density, so we are making further investigation to find other factors of corrosion.

1B16: Characterization of corrosion products in iron in aqueous solutions by in-situ Mössbauer spectroscopy

Sakai, Y., Ohshita, K., Yoshida, M. (Daido Inst. Tech.)

Chemical characterization was carried out for corrosion products on iron metal or steel by transmission ^{57}Fe Mössbauer spectroscopy. The Mössbauer spectra at room temperature were measured in situ for steel wool immersed in water and aqueous solutions of NaNO_3 and NaCl with a concentration of 0.6 M. The measurement set-up was very simple; 95 mg of steel wool with a thickness-diameter of 40 micrometer was put in a polyethylene bag together with the solution. It was revealed from the observed Mössbauer parameters that main corrosion products were magnetite (Fe_3O_4) and lepidocrocite ($\gamma\text{-FeOOH}$) in water, NaNO_3 -, and NaCl -aqueous solutions. The corrosion was observed to proceed slower for the solution of NaNO_3 than for water and the solution of NaCl .

1B17: Mössbauer spectroscopy of transition metal complexes with dihydroxybenzoquinone derivatives

Takao, T., Tooyama, Y., Fujii, S., Sakai, H. (Faculty of Science and Engineering, Konan Univ.)

Mössbauer spectra and X-ray powder diffraction patterns have been measured for iron and iron-doped zinc complexes with 2,5-dibromo-3,6-dihydroxy-1,4-benzoquinone and 2,5-diiodo-3,6-dihydroxy-1,4-benzoquinone. These results are compared with those for the iron complexes with 2,5-dihydroxy-1,4-benzoquinone and 2,5-dichloro-3,6-dihydroxy-1,4-benzoquinone in our previous work. The relationship between the crystal structure of the complexes and the electronic structure of the metal center is discussed.

1B18: ESR spectra of transition metal complexes with dihydroxybenzoquinone derivatives

Tooyama, Y., Takao, T., Fujii, S., Sakai, H. (Faculty of Science and Engineering, Konan Univ.)

Cu^{2+} - and Mn^{2+} -EPR spectra have been measured for copper- and manganese-doped zinc complexes with dihydroxybenzoquinone derivatives such as 2,5-dihydroxy-1,4-benzoquinone, 2,5-dichloro-, 2,5-dibromo-, and 2,5-diiodo-3,6-dihydroxy-1,4-benzoquinone, which consist of coordination polymers. EPR parameters, g and A for the Cu^{2+} ion and zero magnetic splitting D for the Mn^{2+} ion, are discussed in regard to the structure of the coordination polymers.

1B19: Electromagnetically Induced Transparency (EIT) for nuclear gamma radiation via nuclear level-crossing on FeCO_3 single crystal

Muramatsu, H. (Shinshu Univ., IKS-K.U.Leuven), Gheysen, S., Vyvey, K., Coussement R., Odeurs, J. (IKS-K.U.Leuven), Shakhmuratov, R. (Kazan Phys. Tech. Inst., IKS-K.U.Leuven)

We present the first steps towards a proof-of-principle experiment, demonstrating EIT with gamma radiation for the Mössbauer effect in the mineral siderite FeCO_3 . A strong temperature-dependent internal magnetic field parallel to the EFG-axis in the single crystal allows for crossings in the nuclear level structure of ^{57}Fe . Even when we have not applied an external magnetic field, the Mössbauer spectra already show a reduced absorption around the level crossing temperature. A possible explanation would be the existence of inhomogeneities in the crystal inducing a mixing interaction, bringing us in the EIT regime. In order to explain the misfits as the induced transparency at temperatures near the crossing region, the mixing occurred should be large. In comparison with the thick and thin sample, we see a large misfit in the thick sample and a smaller misfit in the thin sample. It is not clear at this stage whether a small misfit in the thin sample is ascribed to the existence of oxide lines, or there exists certain physics in the observed difference. From a measurement in the external magnetic field of 0.5T, no drastic change was observed as far as the degree of misfit is concerned.

1B20:Chemical behavior of energetic hydrogen isotopes implanted into SiC

OYA,Y., KAWAAL,K., MORITA,K., IINUMA,K., OKUNO,K., TANAKA,S., MAKIDE,Y.
(RI center, Univ. of Tokyo, Graduate School of Eng., Nagoya Univ., Graduate School of Eng.,
Tohoku Univ., Graduate School of Sci. & Eng., Shizuoka Univ., Graduate School of Eng.,
Univ. of Tokyo)

The retention and re-emission behaviors of hydrogen isotopes implanted into SiC have been studied by means of elastic recoil detection (ERD) technique. The deuterium ions were implanted into SiC sample at room temperature up to almost the saturation. The isothermal annealing was applied to the deuterium implanted SiC sample and the decay curve of the retention was evaluated and compared with the TDS spectra. It was found that deuterium re-emission takes place in three stages, which were ascribed to the re-emission of Si-D compounds, deuterium molecules formed by recombination of deuterium atoms bound to Si and C in SiC, respectively. The mass balance equations were also used to evaluate the effective molecular recombination rate constant, which was determined to be 7.3×10^{-5} .

1B21:¹⁵⁵Gd Mössbauer spectra and crystal structures of Gd(III) complexes with polyethylene glycols

NISHIMURA, T., TAKAHASHI, M., TAKEDA, M. (Faculty of Science, Toho University)

Polyethylene glycols (PEG) are much flexible polyether compared to crown ethers and can form the complexes having high coordination number with rare earth metals (REE). In this study we have carried out X-ray structural determinations and ¹⁵⁵Gd Mössbauer measurements for PEG complexes of REE; The crystal structures for [Gd(NO₃)₃(2Gly)(H₂O)], [Gd(NO₃)₃(3Gly)], [Gd(NO₃)₃(EO4)], [Gd(NO₃)₂(EO5)](NO₃) and [Gd(EO5)(H₂O)₃](ClO₄)₃ are determined. All the nitrates are 10 coordinated though the numbers of oxygen atoms in PEGs are different. The 10 coordination is achieved by changing the coordination mode of nitrate ligand (bidentate, unidentate or non-coordination). In contrast to nitrate salts, [Gd(EO5)(H₂O)₃](ClO₄)₃ is obtained starting from Gd(ClO₄)₃. The ¹⁵⁵Gd Mössbauer spectra for EO4 and EO5 complexes show that there are some difference in e^2qQ value; 3.53 mm s⁻¹ for EO4 complex and 4.34 mm s⁻¹ for EO5. This can be interpreted by the difference in position of the nitrate ion in the coordination.

1B22:No aptitude of some newspaper accounts for an accident in RI utilization facility.

Asano,T. (Res. Inst. Adv. Sci. Tech., Osaka Pref. Univ.)

On 4. April 2002 an accident was happened in a RI utilization facility of the institute of a private company. The accident was an explosion in an exhaust gas pipe of combustion apparatus specially designed for liquid scintillation counting - organic liquid waste. The use of the combustion apparatus was permitted in the Law Concerning Prevention of Radiation Hazards Due to Radioisotopes, etc. Some newspaper accounts were written as an explosion of exhaust of combustion furnace of general radioactive organic liquid waste, and were not courteous and not educational in expression of radiation exposure and the use of radioisotopes for investigation. Here some appropriate expression will be shown with respect to the accounts of accident, and the importance of diffusion of an accurate knowledge about radiation and radioisotopes for mass media persons, the public and students.

1B23:Newspaper terms such as “the nuclear power peninsula”

Murabayashi, K., Aratani, M*(NPO EGG, IES*)

Where is the nuclear power peninsula in Japan? "Please do not call the Peninsula Shimokita as the nuclear power peninsula. How should I explain it for our children? We cannot find the nuclear power peninsula on any maps." The contribution was carried on the newspaper read widely in Aomori District. For example, we know Kyushu is called as the Silicon Island after the Silicon Valley in USA. They mean names of island or place as special regions derived from their highly technological industries characteristic of the districts. On December 8 of 1983, the Prime Minister Nakasone gave a suggestion that a new base for nuclear power development should be constructed in the Peninsula Shimokita, and as a result the residents committed themselves to the development of nuclear power in pursuit of their own fruitful future. Since then the development has been called as Mutsu Ogawara Development derived from the name of the place. The contributor perhaps may not be proud of it as an important place for energy development in Japan. The background of the naming of it will be discussed and reported.

1C01:Electric reduction of valuable metals in AOT reverse micelles

SHIMIZU, R., TOMIOKA, O., ENOKIDA, Y. (Research Center for Nuclear Materials Recycle, Nagoya University), YOSHIDA, Z. (Advanced Science Research Center Japan Atomic Energy Research Institute), YAMAMOTO, I. (Department of Nuclear Engineering, Nagoya University)

Reverse micelle was formed by mixing of *n*-dodecane, AOT (sodium bis(2-ethylhexyl) sulfosuccinate) and an aqueous solution containing $\text{Cu}(\text{NO}_3)_2$. The particle size and electrical conductivity of this micelle were measured by DLS-7000 (Ostuka Electronics Co.) and MPC227 (Mettler Toledo Co.). With increase of W value, the particle size increased logarithmically and the electrical conductivity showed the maximum value. With cyclic voltammetry, electrolysis reactions in the micelle containing 0.1 mol/l $\text{Cu}(\text{NO}_3)_2$ aqueous solution was measured by a potentiogalvanostat HZ-3000 (Hokuto Denko Co.). A well-defined voltammogram for the redox reaction showed that electro reduction of Cu^{2+} to Cu occurred. Electrolysis was conducted at the reduction potential, 308 K under the static condition for 30 min and 2.2 μg of Cu metals were deposited. This study has demonstrated that Cu metals can be deposited stably from AOT reverse micelles containing Cu^{2+} when regulating acid and Cu^{2+} concentration are adequate. This method is applicable to recover other useful metals from organic solution containing reverse micelles.

1C02:Solubility of uranyl nitrate-TBP complex in supercritical CO_2

TOMIOKA, O., ENOKIDA, Y. (Research Center for Nuclear Materials Recycle, Nagoya Univ.), YAMAMOTO, I. (Department of Nuclear Engineering, Nagoya Univ.)

Extraction of uranium is required for initial production of nuclear fuel, reprocessing of spent fuel and decontamination of uranium waste. Supercritical fluid extraction techniques have been reported for recovering uranium using supercritical CO_2 medium containing HNO_3 -TBP complex as a reactant. But the nature of this complexant system in supercritical CO_2 is not totally understood. The phase equilibrium data was necessary to acquire. In this study, the dew point of uranyl nitrate-TBP complex in supercritical CO_2 was observed by the Phase Equilibrium Analyzer (PEA) system, which equipped a variable volume high-pressure view cell. PEA system measured the pressures and the temperatures of changing to the single phase of the mixture of supercritical CO_2 and the uranyl nitrate-TBP complex, which of the uranium concentration of 0.5 M and 1 M. It is found that the mixture was single phase in more than this pressure. This pressure was increased with an increase of uranium concentration in the complexes. The highest pressure was required at the mole fraction of TBP of the mixture was ca. 0.06.

1C03: Study on the separation of trivalent actinoids from trivalent lanthanoids using electrophoresis

Ishii, Y. (Grad. Sch. Sci. & Tec., Shizuoka Univ.), Yanaga, M., Suganuma, H., (Fac. Sci., Shizuoka Univ.), SATOH, I. (IMR, Tohoku Univ.)

It was tried to separate trivalent actinoids (^{241}Am) from trivalent lanthanoids ($^{152,154}\text{Eu}$) in mixed solvent ($\text{CH}_3\text{OH}/\text{H}_2\text{O}$) solutions using electrophoresis. The concentrations of ^{241}Am and $^{152,154}\text{Eu}$ are tracer scale. The solution consists of (0.1 M HClO_4 + $x\text{M NaClO}_4$) mixed solvent ($\text{CH}_3\text{OH}/\text{H}_2\text{O}$), containing ^{241}Am and $^{152,154}\text{Eu}$. The obtained results showed for a mutual separation of ^{241}Am and $^{152,154}\text{Eu}$ in high ionic strength solutions ($x > 1$) of mixed solvent ($\text{CH}_3\text{OH}/\text{H}_2\text{O}$) to be possible by electrophoresis.

1C04: Sorption of Am(III) and Eu(III) by hematite in the presence of humic acid: Effects of ionic strength

Sakuragi, T., Sato, S., Kozaki, T. (Graduate School of Engineering, Hokkaido Univ.) Mitsugashira, T., Hara, M., and Suzuki, Y. (Oarai Branch, Institute for Materials Res., Tohoku Univ.)

The sorption of Am(III) and Eu(III) in ternary systems consisting of metal ions(III), humic acid, and hematite was studied as a function of ionic strength over a pH range from 4 to 10. Sorption behavior of Am(III) was similar to that of Eu(III). In the absence of humic acid, the Am(III) sorption increased with increased pH and was not affected by varying ionic strengths. In the presence of humic acid, the almost all of Am(III) sorbed on hematite at whole pH regions and an ionic strength of 0.5 M. As the ionic strengths in the system decreased, the Am(III) sorption in the ternary systems decreased with increasing pH above 5.5. The decrease with ionic strengths was similar to the adsorption of humic acid alone on hematite. In order to discuss the sorption behavior of Am(III) in the ternary systems, additivity model was tested using the individual interactions between respective components.

1C05: Carbonate complexation of Np(IV) in alkaline solutions

Kitamura, A., Kohara, Y. (JNC, IDC)

The solubility of Np(IV) in carbonate media under reducing conditions was studied. The concentration of dissolved Np(IV) was measured with ionic strengths of 0.5, 1.0, 2.0 and 2.9 M ($M \equiv \text{mol} \cdot \text{dm}^{-3}$), hydrogen-ion concentration exponent ($\text{pH}_c = -\log [\text{H}^+]$) from 8 to 13 and with the total carbonate concentration (C_T) from 5×10^{-3} M to 0.7 M by an oversaturation method. A reducing agent used was sodium dithionite. It was found that the solubility of Np(IV) increased with increasing C_T . In highly alkaline solutions, the coordination number of carbonate ion for the dominant species of Np(IV) was considered to be 2, on the basis of proportionality between the logarithm of dissolved Np(IV) concentration and $\log C_T$ with a slope of 2. It was also found that the difference between the total neptunium concentration and the concentration of TTA(thenoyltrifluoroacetone)-extracted neptunium suggested the existence of polymeric species of neptunium. Based on the results, the equilibrium constants of the carbonate and/or carbonatohydroxo complexes were obtained. A method for the determination of equilibrium constants only for monomeric species of neptunium will be discussed.

1C06: Structural study of Th metallofullerene

Akiyama, K. (JAERI), Sueki, K. (Tsukuba Univ.), Tsukada, K. (JAERI), Haba, H. (RIKEN), Asai, M. (JAERI), Ichikawa, S. (JAERI), Kikuchi, K. (Tokyo Metropolitan Univ.), Ohtsuki, T. (Tohoku Univ.), Nagame, Y. (JAERI), Katada, M. (Tokyo Metropolitan Univ.), Nakahara, H. (Tokyo Metropolitan Univ.)

For the metallofullerenes of U, Np, and Am, the oxidation states of the encapsulated

actinide atoms and the most abundant species in the crude extract were found both similar to those of the light lanthanide metallofullerenes of La, Ce, Pr, while for the metallofullerene of Th and Pa, the most abundant species in the extract were $M@C_{84}$. The case that the most abundant metallofullerene is not $M@C_{82}$ is rare. Thus, the electronic and molecular structure of this $M@C_{84}$ are of great interest. In this symposium, we will report that the structure assigned by ^{13}C -NMR spectroscopy of the $Th@C_{84}$. The sharp 11 signals assigned to the metallofullerene were observed in the ^{13}C -NMR spectrum of $Th@C_{84}$. The structure of C_{84} fullerene that shows 11 NMR signals is limited to only two kinds of D_{2d} symmetry.

1C07:HPLC behavior of actinoids metallofullerenes

Akiyama, K. (JAERI), Sueki, K. (Univ. of Tsukuba), Tsukada, K. (JAERI), Haba, H. (JAERI), Toyoshima, A. (Osaka Univ.), Asai, M. (JAERI), Ichikawa, S. (JAERI), Kikuchi, K. (JAERI), Nagame, Y. (JAERI), Katada, M. (Tokyo Metropolitan Univ.), Nakahara, H. (Tokyo Metropolitan Univ.)

The formation of metallofullerenes has been reported for alkaline earth, rare earth and group-4 elements. We reported the results of the HPLC study on actinide fullerenes (Th, Pa, U, Np, and Am) using radiotracers. In this work, we will report the results of production and of the HPLC study on actinium fullerene. It is found that actinium fullerene is produced by dc-arc method and has mainly one specie from HPLC behaviors. The specie is able to encapsulate C_{82} from retention time of 5PBB column. But, the actinium fullerene is not similar to $La@C_{82}$ (major), because the retention time of actinium fullerene is faster than that of $La@C_{82}$ on Buckyrep column.

1C08:Complex formation of uranium (VI) with phosphate ion in aqueous solution at high temperatures and pressures

Kirishima, A. (Grad. School of Engineering, Tohoku Univ.), Kimura, T. (Japan Atomic Energy Research Institute), Tochiyama, O. (Tohoku Univ.), Yoshida, Z. (JAERI)

Complexation studies of actinides at high temperatures and pressures are important to predict their migration behavior in natural systems. As a basis of them, the complex formation of U(VI) with phosphate ion has been studied at elevated temperatures (20 ~ 150 °C) and pressure (40 MPa) using time-resolved laser-induced fluorescence spectroscopy. Emission spectra and lifetimes of 5×10^{-5} M uranium(VI) in $NaClO_4$ solutions in the presence and absence of phosphate ion were measured as a function of pH, ligand concentration and temperature. Three components with different lifetimes were observed in the fluorescence decay curves. The spectroscopic results were compared with speciation calculations at several temperatures by using the DQUANT equation and thermodynamic data in the literature. The decay curves were resolved to be composed of three components of fluorescent species corresponding to UO_2^{2+} , $UO_2H_2PO_4^+$ and $UO_2(H_2PO_4)_2$ respectively. The Arrhenius plots of the temperature dependence of the decay constants show high linearity and give following their activation energy and lifetime at 20 °C and 40 MPa. UO_2^{2+} ; $2.3 \pm 0.6 \mu s$, $45.1 \pm 0.5 kJ/mol$; $UO_2H_2PO_4^+$; $15.4 \pm 5.0 \mu s$, $47.8 \pm 0.7 kJ/mol$; $UO_2(H_2PO_4)_2$; $94.6 \pm 14.0 \mu s$, $48.1 \pm 0.3 kJ/mol$.

1C09:The resonance Raman effect of uranyl bond

Soga, T (Japan Atomic Energy Research Institute)

The resonance Raman scattering spectra of uranyl compounds, $UO_2(NO_3)_2$, $UO_2(CH_3COO)_2$, UO_2Cl_2 , $CsUO_2(NO_3)_3$ and $Cs_2UO_2Cl_4$, in dimethyl sulfoxide, $(CH_3)_2SO$, have been measured under laser excitation of the UO_2^{2+} ion in resonance with the $^1\Sigma_g^+ \rightarrow ^1\Phi_g$ electronic transition. The resonance Raman excitation profiles of the totally symmetric stretching vibrational mode of uranyl are presented and analyzed in terms of transform theory within the non-Condon model. It is found that, in the $^1\Sigma_g^+ \rightarrow ^1\Phi_g$ electronic

transition, elongation of the U-O equilibrium bond length is related to the magnitude of the change in the excitation profile and has a linear correlation with the increasing in the charge transferred from the ligand to the uranium atom.

1C10: Synthesis and properties of neptunyl(V) propionates

Nakada, M., Nakamoto, T., Yamashita, T., Masaki, N. M., Krot, N. N. *, Saeki, M. (Jpn. At. En. Res. Inst. *Rus. Acad. Sci.)

From propionate containing solutions of Np(V), the crystalline compounds $\text{NpO}_2\text{OOCCH}_2\text{H}_5/n\text{H}_2\text{O}$ with $n=1$ or 2 and $\text{M}(\text{NpO}_2)_2(\text{OOCCH}_2\text{H}_5)_3/\text{H}_2\text{O}$ with $\text{M}=\text{NH}_4$ or Cs were synthesized. The solids were studied using X-ray diffraction and Moessbauer method. Their behavior upon heating were also studied. The IR and absorption spectra suggest that the neptunyl ions are coordinated with each other to form cation-cation bonds in the compounds. Experimental results also suggest that Np atoms have pentagonal bipyramidal coordination polyhedra and nonequivalent sites of NpO_2^+ exist in them.

1C11: Elution chromatography separation of lanthanides by using anion exchange resin

Ikeda, A., Aida, M., Suzuki, T., Fujii, Y. (Res. Lab. Nucl. Reactors, Tokyo Tech.)

For the purpose of mutual separation of lanthanides, the elution chromatography separation has been carried out by using tertiary pyridine type anion exchange resin in hydrochloric acid-methanol mixed medium. The lanthanides have been separated mutually in $8.2 \text{ mol/dm}^3\text{-HCl} / 30\% \text{-MeOH}$ or $5.9 \text{ mol/dm}^3\text{-HCl} / 50\% \text{-MeOH}$, although they have not separated in $5.9 \text{ mol/dm}^3\text{-HCl} / 30\% \text{-MeOH}$. There was no effect of flow rate on the separation, and it became difficult to separate the lanthanides as the temperature increased.

1C12: Separation of uranium from solid samples by supercritical carbon dioxide leaching method

Meguro, Y., Iso, S., Yoshida, Z., Ougiyangi, J.¹, Enokida, Y.², Yamamoto, S.³ (Advanced Science Research Center, JAERI, Faculty of Science, Ibaraki Univ.¹, Research Center for Nuclear Materials Recycle, Nagoya Univ.², Chemical & Environmental Technology Laboratory, KOBELCO³)

A supercritical CO_2 leaching (SFL) method was developed for the separation of uranium from a solid sample contaminated by uranium oxide. Supercritical CO_2 medium containing a $\text{HNO}_3\text{-TBP}$ complex as a reactant was used. More than 99% of UO_2 or U_3O_8 was leached and recovered from synthetic sand samples (ca. 50 g, 20-30 mesh) contaminated by ca. 100 mg UO_2 or U_3O_8 by the recommended SFL procedure using the $\text{HNO}_3\text{-TBP}$ complex of HNO_3 (4.5 mole) + TBP (3 mole) + H_2O (1 mole) at 60°C and 333 MPa. Only 0.2% of uranium was remained in the sample. From a synthetic porous alumina brick (ca. 8 g) contaminated by 100 mg U_3O_8 , 90% uranium and 70% thorium as a daughter nuclide of ^{238}U (ca. 1 μg) were leached. Pressure pulse performance was effective for the enhancement of the mass transport in a solid sample of high porosity.

1C13: Basic studies of radioactive disequilibrium in U and Th decay series using electrodeposited sources

Morimoto, T., Banba, S., Shinoda, Y., Ishikawa, K. (Japan Chemical Analysis Center), Hashimoto, T. (Depart. of Chem., Fac. of Sci., Niigata Univ.)

During alpha-decay process, the residual or recoiled daughter nuclide might be transferred from its parent position to a new site. In this study, the authors try to get quantitative information of the alpha-recoil atoms using ^{232}U or ^{226}Ra (having descendants). The ejection and injection behavior of recoil atom ^{224}Ra from its parent ^{228}Th or ^{222}Rn from its parent ^{226}Ra were investigated on both source and collector. A spacer (0.1mm thickness) having a

hole of 5mm diameter was inserted between the electrodeposition source and the collector. The assembly was stored in a vacuum chamber of about 1.3 Pa. After the exposure, the collectors were measured by alpha-spectrometry to determine the activity strength. In the case of Th-decay series, the spectrum showed the alpha-spectrum due to ^{224}Ra along with their daughters on the collectors. These findings show that ^{224}Rn is ejected from ^{228}Th source and moved to the collector owing to recoil behavior. Generally, the injection factors in inorganic material collector gave higher ratios in comparison with in organic materials.

1C14:Uranium isotopic composition in lake sediment and sedimentary environment: Lake Kawaguchi in Fuji-Goko

¹Yamamoto, M., ¹Shimizu, T., ¹Sakaguchi, A., ²Sasaki, K., ³Koshimizu, S., ¹Komura K. (¹LLRL, ²KGU, ³YIES)

The sediment cores from Lake Kawaguchi in Fuji-Goko, Yamanashi Pref., were analyzed for U and its isotopic ratio, with the measurements of ^{210}Pb and ^{137}Cs and elemental compositions. The lake is a eutrophic. In three core sediments (30-40 cm depth) analyzed, particularly the ^{238}U concentrations changed every sampling sites and the $^{234}\text{U}/^{238}\text{U}$ activity ratios were observed to vary from 1.11 to as high as 1.59. For one core sediment, its ratios seem to decrease with depth. Such high ratios in the core sediments are attributable to authigenic U in the lake water. The ^{238}U concentration and its $^{234}\text{U}/^{238}\text{U}$ activity ratios in this lake water were ca. 0.1 mBq/L and 1.6, respectively. The factors controlling behavior of deposition of U are mainly discussed.

1C15:Detection of U-disequilibrium in phosphate fertilizer

Abe, T., Asayama, N., Kazama, K., Sasaki, K. (Chemistry Department, Rikkyo University)

We observed a large disequilibrium between U-234 and U-238 in a commercial phosphate fertilizer. The sample fertilizer was ground, dried and leached in a plastic column successively by using water, 0.1 M HCl, and 8 M HCl. Finally, the residue was leached with a mixture of hydrofluoric acid, nitric acid and perchloric acid in a pressurized PTFE container. The ratio of U-234 / U-238 radioactivities amount to 8.1+/- 1.6 in the final fraction of successive leaching steps. The other leachate fractions showed little disequilibrium, where the ratios were around 1, and the average value was 1.00+/- 0.02. It should be noted that the overall U-234 / U-238 radioactivity ratio was 1.7+/- 0.1 and that ca 50% of U-234 was found in the final leachate in contrast to the results on ordinary apatite minerals. The large disequilibrium may be caused through the industrial processes to make fertilizer.

1C16:Rapid determination of long-lived nuclides in environmental samples using time interval analysis

UEZU, Y^{*1}. and HASHIMOTO, T^{*2}. (^{*1}Japan Nuclear Cycle Development Tokai Works, Faculty of Science Niigata University^{*2})

It is well known that the environmental monitoring, discharge monitoring into the environment and working place monitoring of long lived alpha nuclides, including plutonium, are very important because of biologically radiation effects when intake in human body. So, this monitoring is needed a very sensitivity. In such high sensitivity monitoring, natural radionuclides, including radon (Rn) and its decay products, should be eliminated as low as possible. In this situation, a sophisticate discrimination method between Pu and decay products of Rn using time interval analysis (TIA) was developed. In simulation experiments, when fixed time intervals for correlated event (decay products of Rn) extraction were varied from 0.1 to 100 milliseconds, it was found that both single time interval analysis (STA) and multiple time interval analysis (MTA) method could subtract satisfactorily short half-life

nuclides within 1 milliseconds and 100 milliseconds orders, respectively. Furthermore, occurring probability of correlated events was set to 0.2, the higher limit of detectable count rate of long-lived nuclides for example Pu were evaluated to be several counts per second by STA method. The using of MTA method was found to be no higher limit of counting rate for long-lived nuclides. On the other hand, the lower limit of determination of Pu-239 is calculated as approximately 6×10^{-9} Bq/cm³. The discrimination system between Pu and other short-lived nuclides using STA or MTA method is concluded to be especially useful for low concentration screening of Pu in dust samples. After screening, more accurate determination of long-lived alpha nuclides would be performed using chemical separation procedure such as anion exchange and/or solvent extraction.

1C17:Lead isotope ratios and source identification of aerosols collected at Jeju, Korea

Oh, Y. (Cehju National Univ., Kyushu Univ.), Kawamura, H. (KEEA), Tennichi, Y. (KEEA), Matsuoka, N. (KEEA, Kyushu Univ.), Maeda, Y. (Kyushu Univ.).

We identified the source of lead in aerosols collected at Jeju, Korea, by comparing lead isotope ratios ($^{207}\text{Pb}/^{206}\text{Pb}$, $^{208}\text{Pb}/^{206}\text{Pb}$) of aerosols with those of local source materials, such as vehicle exhaust, fly ash from refuse incinerator and soil. Samplings were carried out from 8 to 17 April 2002. The samples were pretreated by microwave digestion and the ratios were determined by using ICP-MS, followed by normalization with NIST SRM981.

1C18:Radioactivity of atmospheric aerosol and deposition in Kumamoto city

Kusano, Y., Nishio, S. (Grad. Sch. Sci. Tech., Kumamoto Univ.), Toyoshima, T., Momoshima, N. (Fac. Sci. Kumamoto Univ.)

Many radioactive-nuclides adhered to aerosol are existing in the atmosphere such as ^{210}Pb and ^7Be are removed from the atmosphere as atmospheric deposition. Rain is one of the most effective pathways to remove the aerosol from the atmosphere. Concentrations of ^7Be and ^{210}Pb in each rain sample were measured for 35 samples collected from June 2001 to April 2002 at Kumamoto, Japan. The concentrations of ^{210}Pb and ^7Be were 14.2 ~ 672.0 mBq/L, 117.0 ~ 2931.2 mBq/L, respectively. The concentrations of ^{210}Pb and ^7Be in atmospheric aerosol were measured for 20 samples collected from November 2001 to May 2002. The concentrations of ^{210}Pb and ^7Be were 1.7 ~ 20.4 mBq/m³, 5.7 ~ 91.8 mBq/m³, respectively. The higher concentrations of ^{210}Pb and ^7Be in rain samples were observed at low precipitation and decreased with precipitation. This tendency is also observed on the cases for radioactive concentrations of atmospheric aerosol, indicating that dry deposition and wash out are the major contributors at low precipitation and rain out shows a larger contribution at high precipitation.

1C19: ^{137}Cs in recent fallout samples in relation to the Asian Continent aerosols.

ISHIKAWA, Y., SAGA, K. (Environ. Radioact. Res. Inst. Miyagi), NARAZAKI, Y. (Fukuoka Inst. Health & Environ. Sci.), YAMAZAKI, K., TANABE, H. (Niigata Pref. Inst. Pub. Health & Environ. Sci.)

^{137}Cs in rain and dry fallout samples was investigated in Miyagi, Niigata and Fukuoka Prefs., Japan. Large amount of ^{137}Cs deposition was observed immediately after the Chernobyl accident in 1986, though the values decreased rapidly. In 1990's, about 0.03-0.5 Bq/m² of ^{137}Cs has been often observed until 1996, and after that ^{137}Cs was rarely observed till the end of 1999. However, since 2000, ^{137}Cs deposition increased again, probably because of the Asian Continent aerosols. This was confirmed by observations of ^{137}Cs in the aerosol samples in Miyagi and Fukuoka Prefs., collected after the dust storms in the Continent using by high-volume air samplers.

1C20: Variations of Be-7 and Pb-210 concentrations in atmosphere on rain events

Kameda, S., Sugihara, S., Osaki, S*, Maeda, Y. (Graduate School of Science, Kyushu Univ., *Radioisotope Center, Kyushu Univ.)

Variations of Be-7 and Pb-210 concentration in atmosphere on rain events were measured to study about influence of meteorological factor on aerosol scavenging in atmosphere. Samples were collected at Kyushu University in Fukuoka City. Be-7 and Pb-210 concentrations in atmosphere decreased when rain started and it increased when rain ended. These variations showed that aerosol was scavenged from atmosphere with rain, and Be-7 and Pb-210 concentrations in atmosphere recovered to the levels before rainfall. Be-7 and Pb-210 deposition rates per precipitation decrease with raining. These variations show that in scavenging process washout was more dominant than rainout at the early time of rainfall.

1C21: Measurement of dry deposition rates on grasslands and forests by use of environmental radioactivities

Maruta, M. Sugihara, S. Osaki, S. Maeda, Y. (graduate school of science, kyusyu univ.)

Dry deposition rates are very important to know the incoming of pollutants to the ecosystems. But it is very difficult to estimate the dry deposition rates on practical grasslands and forests because of the difficulty on the distinction of dry deposition rates from wet deposition rates. The half-life of ^{212}Pb is 10.6h. So the concentrations of ^{212}Pb only reflect before 2 days' history. If it doesn't rain for longer than 3 days, it is possible to estimate the dry deposition rates by use of the environmental radioactivity of ^{212}Pb . 70% of Japanese land is covered with forests. It is important for all ecosystems to develop the dry deposition rates of the transfer substance. In order to solve the systems of aerosol removal, we have measured dry deposition rates of particles on grasslands and forests by use of environmental radio-activities.

1C22: An attempt to measure radiation doses using radioactive aerosols

Oki, Y., Takamiya, K., Shibata, S. (Research Reactor Institute, Kyoto Univ.)

A new method for radiation dose measurement in radiation facilities, such as high energy and high intensity accelerators, was proposed. In this method, activation or physico-chemical property changes of fine particles in radiation fields are applied to the dose estimation. A tube is installed in a radiation field inside the accelerator tunnel. During operation of the accelerator, the particles are introduced into the radiation field through the tube from the outside of the tunnel as aerosols, and are irradiated with radiation. The irradiated aerosols are collected at the outside of the tunnel, and their activity or the property change is measured. In this work, we focused on the background and theoretical aspects of this method, and discussed its feasibility.

3A01: Radiochemical study of manganese concentration and its uptake behavior in brain — their changes in fetal, suckling and developmental mice —

Tsuji, T., Hirunuma, E*, Enomoto, S*, Amano, R. (School of Health Sciences, Faculty of Medicine, Kanazawa University. *The Institute of Physical and Chemical Research (RIKEN).)

To gain a comprehensive understanding of the biological function and behavior of manganese (Mn), the elemental concentration, uptake behavior and retention of Mn were studied using neutron activation analysis (NAA), multitracer (MT) and autoradiography methods, respectively, in the brains and other organs (parietal bone, liver, spinal cord) of the fetus, suckling (~3 weeks) and developmental (4~7 weeks) mice. As a result, the Mn uptakes by the brain and spinal cord were found to be significantly higher than those of the other organs in the fetal and suckling periods, although the Mn concentrations was low

(0.15ppm). Brain Mn concentration was found to increase with development and remain constant (0.47ppm). In addition, we found the other following facts: (1) The biological half-life of ^{54}Mn in brain was long. (2) Injected ^{54}Mn was transported into brain via choroid plexus. Mn should play an important role in the brain development

3A02: Biodistribution of neptunium 4n+1 decay-chain nuclides in mice.

Washiyama, K., Amano, R., Kinuya, S. (Fac. Med., Kanazawa Univ.)

Shiokawa, Y. (Institute for Material Research, Tohoku Univ.)

Alpha-ray from heavier elements than $Z=82$ are of considerable interest for tumor-therapy in nuclear medicine due to its high-LET and short range in comparison with beta-ray. Moreover, these alpha-ray emitted nuclides are member of decay chain nuclides. These decay chain nuclides are more potential for tumor therapy than single alpha-, beta-, gamma-particle emitted nuclides. Therefore, it is necessary to investigate their chemical speciation *in vivo* and biodistribution of mother and daughter nuclides after decay cascade. In this study, we evaluated biodistribution of neptunium series nuclides, ^{225}Ra , ^{225}Ac , ^{213}Bi which emits alpha particles after their disintegrations. Three groups of ICR male, 8-week-old, mice were administered ^{225}Ra , ^{225}Ac , ^{213}Bi . After appropriate time intervals, the liver, kidney, spleen, femur, blood and urine are excised and subjected to gamma-ray spectrometry. As the results, there are various accumulation patterns of daughter nuclides after administration of the 3 different nuclides. Although almost ^{225}Ac were accumulated in liver after ^{225}Ac injection, ^{225}Ra and daughter ^{225}Ac were almost remained in bone of mice injected ^{225}Ra . This difference was explained on the bone seeking property of Ac.

3A03: Protecting effect of tea catechins against the lipid peroxidation induced by gamma-irradiation

Tsuchiya, H., Ohashi, Y., Suzuki, Y., Taguchi, H., Yoshioka, H., Yoshioka, H. (Radiochem. Res. Lab., Fac. of Sci., Shizuoka Univ.¹, Inst. For Environmental Sci., Univ. of Shizuoka²)

Protecting effect of tea catechins, (-)-epicatechin (EC), (-)-epigallocatechin (EGC), (-)-epicatechin gallate (ECg) and (-)-epigallocatechin gallate (EGCg), against the lipid peroxidation induced by ^{60}Co gamma-irradiation was examined using a spin probe, 16-NS. Catechin and 16-NS were incorporated into a liposome prepared from egg yolk lecithin, and the ESR intensity of 16-NS was followed as a function of the irradiation time. Catechin and 16-NS were thought to compete for the scavenging of the lipophilic radicals formed by the irradiation and responsible for the lipid peroxidation. Therefore, 16-NS lives longer if the coexisting catechin has a stronger activity to the scavenging. The difference of the activity of four catechins was discussed from the viewpoints of their molecular structures and the locating positions in the lipid bilayer.

3A04: Dependence of TL property changes on impurities in quartz accompanied with thermal treatment

Yamaguchi, T., Mitamura, N.¹, Hashimoto, T.¹ (Graduate School of Sci. and Technol., Niigata univ., Fac. of Sci., Niigata univ.¹)

The change of TL property from quartz slice and grain samples accompanied with thermal treatment for 100h at 1100°C has been studied on the basis of IR absorption spectrum, α - β transition temperature and ESR spectrum. Consequently, it was noticed that TL signal from thermally annealed quartz enhanced greatly their sensitivities in comparison with the original quartz. In addition, two new TL emission peaks, giving around 380 nm and about 630 nm, appeared at the all parts, in which both BTL and no BTL parts were changed into RTL on the slice after annealing treatment. Concerning the luminescence color changes, the distribution patterns due to OH-impurities from the IR absorption spectra were compared with

the color center images (CCIs) and the TLCIs with and without the thermal treatment. The α - β transition temperatures from colorless (no-CC) part, corresponding to higher impurities part apparently shift toward the lower temperature side around 571.6°C and *vice versa* from original 573°C after thermal treatment. From result of ESR, it was supported that OH-impurities would be playing an important role in radiation-induced phenomena within quartz.

3A05: Sensitivity changes in thermoluminescence (TL) and optically stimulated luminescence (OSL) by annealing treatment of volcanic quartz grains

NAKAGAWA, T. (Graduate school of Science and Technology, Niigata University),
HASHIMOTO, T. (Department of Chemistry, Niigata University)

Dielectric materials such as quartz and feldspar exposed to ionizing radiation exhibit both thermoluminescence (TL) and optically stimulated luminescence (OSL) which are useful for dating. In general, red TL (RTL) is observed from volcanic quartz and artificially burnt quartz grains, so that these quartz could be employed for RTL dating. However, blue-light stimulated luminescence (BSL) signals from volcanic quartz have been recognized to be extremely weak compared with one from burnt quartz such as archaeological potteries and roof tiles. Thus, the BSL signals from burnt quartz were expected to enhance by the annealing treatment, so that the sensitivity changes of the BSL signal associated with annealing treatment were investigated, especially for the volcanic quartz. As a result, significant enhancement of BSL has been confirmed after annealing treatment beyond 700°C together with a slight decrease of RTL-sensitivity.

3A06: Luminescence dating of Jomon pottery and burnt stone from the Okumiomote site, Niigata

Usuda, H., Takano, M., (Graduate School of Science and Technology, Niigata Univ.),
Hashimoto, T., (Faculty of Science, Niigata Univ.)

Some of Jomon pottery and burnt stone from the Okumiomote site, Niigata prefecture, Japan, were applied to luminescence dating. In our laboratory, it has been recognized that volcanic and burnt quartz grains gave red thermoluminescence (RTL) property. A single aliquot regenerative-dose (SAR) method was initially applied to the RTL measurements for these quartz grains. The same quartz grains were also followed to blue-OSL (BSL) dating using the SAR method. All sample preparation was undertaken under subdued red light to prevent affecting the dating signal from quartz. The samples were gently crushed to suitable size with an agate mortar. With the selected sample grains, density separation was carried out to separate quartz. All quartz samples were treated with concentrated HF for 1 hour followed by washing with HCl and water. The annual doses were determined by γ -ray spectrometry for related materials. The final RTL ages evaluated were in excellent agreement with archaeological age estimates, whereas BSL results gave underestimation.

3A07: Identification of volcanic quartz origins from equivalent dose using RTL from a single grain

Yawata, T. (Graduate School of Science and Technology, Niigata University), Nomura, S.,
Hashimoto, T. (Department of Chemistry, Niigata University)

Red thermoluminescence (RTL) phenomena have been initially found in quartz grains, which were extracted from Niigata dune sand, where have been geologically assumed to be the origin of Agano River. The quartz grains from volcanic ash layers have been recognized to give RTL without any exception. As the RTL possesses superior properties with respect to long-time storage of trapped electrons and excellent response nature against doses, the RTL from a single grain will be available to obtain the reliable information in the geological and archaeological fields. In this study, a single grain regenerative-dose (SGR) method has been

developed for residual natural-dose determination using RTL-measurement from each quartz grain, extracted from Niigata. The equivalent doses evaluated from 72 grains were summarized in a histogram expression. From these results, it was confirmed that Niigata dune originates at least from four different volcanic origins. As a result, one of the several origins was identified to be the Numazawa volcano origin, because residual natural dose from single grain method is equal to that of RTL-quartz grains of Numazawa pumice.

3B01: Vertical distribution of elements and their chemical states in Arakawa-river sediment

Kataoka, M., Matsuo, M. (Graduate School of Sci., The Univ. of Tokyo, Graduate School of Arts and Sci., The Univ. of Tokyo)

We collected sediments vertically in Arakawa-river which is located at the east part of Tokyo and the river is assumed to be polluted with the human activities. Using Instrumental Neutron Activation Analysis and Prompt γ -Ray Analysis, we have got vertical distribution of thirty and more elements. Chemical states of iron in the sediments were investigated by Mössbauer spectroscopy. In the vertical distribution of iron species, maximum pyrite distribution was found in the middle layer. On the other hand, paramagnetic high-spin Fe^{3+} distributed complementarily to pyrite, suggesting that the Fe^{3+} was used for pyrite formation. The distribution of pyrite was similar to the sediment of other areas which had different degrees of anthropogenic effects. This fact suggests that pyrite formation in the middle layer of the sediment is not affected by anthropogenic effects. Chemical states of manganese in the sediments were investigated by X-ray absorption fine structure (XAFS), indicating that much manganese sulfide distribution was found in the surface layer.

3B02: Characterization of iron and boron in Asian dusts by Mössbauer spectroscopy and prompt γ -ray Doppler broadening

Sakai, Y., Ohshita, K. (Daido Inst. Tech.), Kubo, M. K. (Intern. Christ. Univ.), Matsue, H., Yonezawa, C. (JAERI)

Chemical characterization of iron and boron was carried out for an Asian dust (called "kosa" in Japanese) sample, which was collected at Nagoya in March 2002. The contents of iron and boron were determined to be 4.4 % and 59 ppm, respectively, by activation analysis using neutron-induced prompt gamma-rays. The chemical states of iron was non-destructively examined by ^{57}Fe Mossbauer spectroscopy, while the boron states was investigated using Doppler broadening effect of prompt gamma-ray. It was proved from the Mössbauer measurements that hematite ($\alpha\text{-Fe}_2\text{O}_3$) and paramagnetic Fe^{3+} - and Fe^{2+} -species exist in the sample. The degradation constant D was estimated to be $1.8 \times 10^{12} \text{s}^{-1}$ for ^7Li moving in the Asian dust sample by analysis of the Doppler broadening line-shape, allowing us to discuss on the physico-chemical environments of the energetic ^7Li produced in the $^{10}\text{B}(n,\alpha)^7\text{Li}$ reaction.

3B03: Iron film produced by laser-evaporation

Matsumoto, K., Hirayama, S., Masukawa, S., Yamada, Y. (Department of Chemistry, Science University of Tokyo)

We have reported the reactions of laser-evaporated iron atoms with various reactant gases, and also found that the spin-orientation of unreacted iron metal is parallel to the substrate surface. It is well known that Mössbauer spectroscopy provides useful information on spin orientation of iron. In this study, we report iron film on aluminum surface produced by laser-evaporation. We measured the sample with various amount of iron. When a small amount of the iron is deposited, iron particles having various sizes are observed as well as $\alpha\text{-Fe}$ metal. On increasing an amount of iron, broad absorption was observed, indicating the distributed magnetic fields of the iron particles with various sizes. We performed curve

fitting assuming the distributed magnetic fields of iron particles, and found that the intensity ratio of peaks is 3:4:1:1:4:3. Therefore the spin of the iron particles are oriented to the parallel to surface. When the amount of iron is further increased, α -Fe metal appears again while broad absorption disappears. It is demonstrated that deposition of laser-evaporated iron produces the film that consists of particles with in-plane spin direction.

3B04:TDPAC studies using probes implanted in powder C₆₀

Sato, W., Ueno, H., Watanabe, H. (RIKEN) Ogawa, H., Miyoshi, H. (Dep. Phys., Tokyo Inst. Tech.) Imai, N. (Dep. Phys., Univ. Tokyo) Yoshimi, A., Yoneda, K. (RIKEN) Kameda, D. (Dep. Phys., Tokyo Inst. Tech.) Kobayashi, Y. (RIKEN) Sueki, K. (Grad. School Sci., Tokyo Met. Univ.) Ohkubo, Y. (Res. Reactor Inst., Kyoto Univ.) Asahi, K. (RIKEN; Dep. Phys., Tokyo Inst. Tech.)

Time-differential perturbed angular correlation (TDPAC) measurements were performed with probes implanted in powder fullerene C₆₀. As probes for the present studies, we have employed ¹⁹F disintegrated from ¹⁹O and ¹⁴⁰Ce, a beta-decay product of ¹⁴⁰Cs. Those parent nuclides were implanted by using the RIKEN projectile fragment separator and isotope separator on line at Research Reactor Institute, Kyoto University, respectively. Two different components are observed in the TDPAC spectra of ¹⁹F in powder C₆₀: one shows slow relaxation of the angular anisotropy and the other has an oscillatory structure implying the nuclear precession. On the other hand, one can see an explicit oscillation in the time spectrum of ¹⁴⁰Ce, reflecting static electric quadrupole interactions. Taking into account the difference in the charge states and the ionic radii between the probes, we discuss the outer surroundings of the probe nuclei through the static and dynamic interactions with C₆₀ molecules.

3B05:Positron lifetimes in the vicinity of critical point of carbon dioxide

Kino, Y., Sekine, T. Tsukakoshi S., Kudo, H. (Tohoku Univ.), Ito, Y. (Univ. of Tokyo) and Suzuki, T. (KEK)

We measured positron annihilation lifetime spectra of carbon dioxide targets in the vicinity of critical point. The spectra obtained were fitted with attenuation functions having three lifetime components. The lifetimes were regarded as a para-positronium decay, a free positron decay and a orth-positronium decay, in order of length. The para-positronium components were almost constant in this measurement. However, the other two components changed dramatically at the boundary line between gas and liquid phase, and changed gradually at the critical isochore. In the present paper, we report relations between positronium lifetimes and the density of the target.

3B06:Positronium formation and positron annihilation cross sections in positron-hydrogen collisions

Kino, Y., (Tohoku Univ.), Yamanaka, N., (RIKEN), Takano, Y., and Kudo, H. (Tohoku Univ.)

We calculate positronium formation and positron annihilation cross sections in positron-hydrogen collisions with the time-dependent coupled channel method. In this method, the time-evolution of wave functions of an electron and a positron are calculated within a full-quantal framework. Moreover, a physical picture of dynamics can be easily obtained through a computer graphics. The calculated positronium formation cross sections are in good agree with experimental values. The calculated positron annihilation cross section has a peak at $E=0.38$ a.u. In the low incident energy region, the annihilation cross section is inversely proportional to the energy. The distribution of annihilation cross section is obtained as a function of the distance between hydrogen nucleus and annihilation point. The distribution is independent of the energy inside the hydrogen atom, because Coulomb

interactions are dominant inside the atom. The distribution outside the atom decreases with the energy.

3B07: Measurements of electronic X-ray spectrum following pion capture process

GOTO, K., KASAMATSU, Y., TAKAMIYA, K., TOYOSHIMA, A., SHOUJI, Y., NINOMIYA, K., KIKUNAGA, H., KINOSHITA, K., YOKOYAMA, A., HAMAJIMA, Y., MIURA, T., SHINOHARA, A. (Grad. School of Sci., Osaka Univ., Res. Reactor Inst., Kyoto Univ., Grad. School of Natural Sci., Kanazawa Univ., Faculty of Sci., Kanazawa Univ., Res. Center of Radiation, KEK)

Some test experiments were carried out for measurements of electronic X rays correlated with pionic X rays in the negative pion capture on molecules. The measurements were done at the pi-miu-channel of KEK-PS. Hf KX rays were observed in a Ta target. A little correlation was found in the change of the electronic X-ray intensities coincident with the relevant pionic X rays. A new experimental method to reveal the atomic process following the pion capture was discussed based on the results of the test experiment.

3C01: Characteristics of low background Ge and Si detectors in Ogoya underground Laboratory

KOMURA, K., HAMAJIMA, Y. (LLRL, Inst. of Nature and Env. Technol., Kanazawa Univ.)

In order to measure extremely low level natural and artificial radionuclides, underground laboratory (270 mwe) was constructed in a tunnel of former Ogoya copper mine located about 20km from LLRL. Eight Ge detectors (coaxial type 93.5% Ge, 4 well type Ge [73%, 70%, 65%, 37%] and 3 planar type Ge [28cm²x2cm, two 38cm²x3cm]) and 300mm²x0.5mm Si \square -ray detector are set in Ogoya underground laboratory. Background of Ge detectors are typically 1~2 orders of magnitude lower than those set in ground level laboratory. It became possible to detect airborne ²¹⁰Pb, ⁷Be in several 10 m³ of air, ¹³⁷Cs in 10 liters of coastal sea water etc. Since 1995, following measurements have been made at Ogoya underground laboratory: cosmic ray induced nuclides in freshly fallen meteorites (1995, 1996, 19899), natural radionuclides induced by environmental neutrons for example ¹⁹⁸Au, ¹⁹²Ir, ¹⁵²Eu, ¹³⁴Cs and ⁶⁰Co, radionuclides induced by the JCO criticality accident in 1999, ¹⁵²Eu and ⁶⁰Co induced by Hiroshima and Nagasaki Atomic Bombing, cosmic-ray induced ²²Na in rain, river and lake waters.

3C02: Recent trend on plutonium deposition observed at Tsukuba

Hirose, K., Igarashi, Y., Aoyama, M., (Meteor. Res. Inst.), C.K. Kim, C.S., Kim, C.K. (KINS)

Plutonium in deposition samples has been measured since 1957 at the Meteorological Research Institute, Japan. After cease of the atmospheric nuclear weapons testing, ^{239,240}Pu in deposition samples decreased until 1985. In the period from 1985 to 2000, no systematic year-by-year change of annual ^{239,240}Pu deposition has been observed. On the other hand, the monthly ^{239,240}Pu deposition shows clear seasonal change with a maximum in spring season, which corresponds to dust season in the eastern Asia. These findings suggest that a significant amount of the current ^{239,240}Pu deposition is originating from the resuspension of ^{239,240}Pu-bearing soil particles, which are produced in Chinese arid regions. In order to elucidate the origin of resuspended ^{239,240}Pu, plutonium isotopic ratio (²⁴⁰Pu/²³⁹Pu atomic ratio) was determined using HR-ICP-MS. The plutonium isotopic ratios (²⁴⁰Pu/²³⁹Pu) in the monthly deposition samples in 1999 ranged from 0.18 to 0.25. The plutonium isotopic ratios in monthly deposition samples in dust season were the same than that in global fallout (0.18).

3C03: Distribution of plutonium at plowed fields in Rokkasho, Aomori.

OHTSUKA, Y., IYOGI, T., KAKIUCHI, H., HISAMATSU, S. & INABA, J. (IES)

The background distribution of Pu in soil was investigated in Rokkasho, Aomori Prefecture, where the first commercial nuclear fuel reprocessing plant in Japan is now constructed. We made an investigation program covering plowed fields, rice fields, orchards, forests and un-cultivated fields year by year. This is the first report for plowed fields. The soil core samples down to 1 m deep were collected at 13 plowed fields in Rokkasho and a control site in Hachinohe and Hirosaki. Since the field under yam (*Dioscorea babatus*) cultivation, which is common in Rokkasho, was dug up to approximately 1 m deep at harvesting, depth profiles of fallout radionuclides were heavily disturbed at the most fields in Rokkasho. The mean and standard deviation of inventory of $^{239+240}\text{Pu}$ in three undisturbed field was 120 ± 50 Bq m^{-2} , and similar to that in Hachinohe. However, the inventory was approximately a half of that in Hirosaki. The mean ratio of $^{240}\text{Pu}/^{239}\text{Pu}$ for all studied fields was 0.18 ± 0.04 , and similar to that of the global fallout. The Pu concentrations very well correlated with ^{137}Cs ($r=0.97$) in spite of heavy disturbance of soil, and the ratio of $\text{Pu}/^{137}\text{Cs}$ was 0.037 ± 0.007 , which is a typical value for global fallout.

3C04:Collection of molecular hydrogen in the air

Sakuma Y. (NIFS), Iida T., Koganezawa T. (Graduate School of Engineering, Nagoya Univ.), TANAKA M. (Japan Air-conditioning Service Co. & Ltd.), OHTA M. (Faculty of Engineering, Niigata Univ.)

This is a basic research for the development of a tritium monitor which measures tritium concentration of molecular hydrogen in the air directly. Molecular hydrogen of about 0.5ppm is included in the air. The tritium concentration is about $25\text{mBq}/\text{m}^3$ -air, and the specific activity is bigger over 5 digits than the vapor in the air. Then the tritium concentration measurement is possible for the easiness, if the molecular hydrogen is collected. The simulated air, consisted of nitrogen 99%, argon 1%, hydrogen 500ppm and methane 500ppm, was prepared. Using a palladium base alloy permeable membrane the experiment which separated the hydrogen from the gas was carried out. The result showed that the pure hydrogen could be efficiently collected.

3C05:Time efficiency of tritium measurement in the environmental water by electrolysis enrichment

Koganezawa, T., Iida, T. (Graduate School of Engineering, Nagoya Univ.), Sakuma, Y., Yamanishi, H. (National Institute for Fusion Science), Ogata, Y. (School of Health Science, Nagoya Univ.), Tsuji, N. (Japan Air-conditioning Service Co & Ltd.), Kakiuchi, M. (Fac. of Science, Gakusyuin Univ.), Satake, H. (Fac. of Science, Toyama Univ.), Torikai, Y. (Hydrogen Isotope Research Center, Toyama Univ.)

Now the electrolysis is necessary for tritium enrichment in Japan. However, the electrolysis needs distilling sample water at before and after the electrolysis. The purpose of this study is to investigate the possibility of more convenient method for tritium measurement. The method substitutes filtration for distillation at before electrolysis and omits distillation at after electrolysis with solid polymer electrode. First, impurities eluted from electrolysis installation were measured. They brought noneffective quenching. Secondly, we applied new method to the environmental waters. Although impurities in the samples by the filtrations were higher than that by the distillation, they brought noneffective quenching. We, however, observed distemper of the electrolysis happened by electrolyzing filtered sample. Distillation is substituted filtration at before enrichment and omitted at after enrichment, leaving the influence of quenching out of consideration.

3C06:A rapid analytical method for ^{129}I determination in environmental samples using an anion exchange resin disk and ICP-MS

Kishimoto, T., Isogai, K., Ohki, Y., Morimoto, T. (Japan Chemical Analysis Center)

^{129}I (half-life 1.57×10^7 y) is an important radionuclide for environmental monitoring around the nuclear fuel reprocessing plant especially in case of emergency. In order to assess the ^{129}I contamination level quickly, a rapid analytical method of ^{129}I in environmental samples using a 3M EmporeTM anion exchange resin disk and ICP-MS has been developed. Known amount of stable iodine (^{127}I) was added to the environmental samples as a yield monitor. ^{127}I and ^{129}I in the sample solution were quantitatively adsorbed with an anion exchange resin disk at flow-rate of 220 ml min^{-1} . The disk was washed with pure-water to remove the matrix elements and then iodine was quantitatively eluted using 1M nitric acid at flow-rate of 9 ml min^{-1} . The separation time required was about 20 minutes. The chemical form of iodine was adjusted to iodate (IO_3^-) by adding sodium hypochlorite solution and determined by ICP-MS. The detection limits of ^{127}I and ^{129}I were 0.1 ng ml^{-1} and 0.7 mBq ml^{-1} , respectively. The full sample analysis process can be achieved within about 12 hours.

3C07: Study on the migration behavior of suspended particles in river waters by using radionuclides as a tracer

Nagao, S*, Ueno, T**, Nagano, T**, Yanase, N**, Tsuduki, K**. (*Graduate School of Environ. Earth Sci., Hokkaido Univ., **Japan Atomic Energy Res. Inst.)

The suspended particles in river waters were collected from the Kuji River waters by a single-bowl continuous-flow centrifuge to study their migration behavior and supply from the watershed. The water samples were taken at a station (9km from the river mouth) from April 2001 to January 2002. The radioactivity of K-40, Cs-137 and Pb-210 was measured by a well-type Ge detector to use a tracer of suspended particles because these radionuclides were present as different forms of soils. The concentration of suspended particles increased with increasing flow rate of river waters. On the other hand, the radioactivity of these radionuclides was divided into two groups. These groups were related to the flow rate of river waters. These results indicate that the migration behavior of suspended particles may be controlled by the flow rate and the precipitation.

3C08: Measurement of low-level cosmogenic ^{22}Na and its application to fresh water system

¹Sakaguchi, A., ¹Yamamoto, M., ²Ohtsuka, Y., ³Sasaki, K., ⁴Yokota, K., ¹Komura, K. (¹LLRL. ²IES. ³KGU. ⁴LBRI.)

^{22}Na is one of the cosmogenic radionuclides. It has, however, been little applied to hydrosphere because its level is extremely low. It might become a useful tracer for evaluating mean residence times of soluble materials in lakes and in drainage basins because Na is conservative element. ^{22}Na was found to be detected by using the ultra low background Ge-detector installed at underground (Ogoya Lab.) .A simple technique was developed to concentrate ^{22}Na by an ion exchange method from water samples (more than 500 L) followed by main components (Ca, Mg, etc.) and K removal procedures. ^{22}Na concentrations in the lake and river waters were measured to be in the ranges of 20-32 and 27-40 $\text{mBq} \cdot \text{m}^{-3}$, respectively. Mean residence times of ^{22}Na in Lake Biwa and its catchment area were estimated to be ca. 11 and 19 years, respectively.

3P01: Determination of multielements in reference materials of sediments by k_0 -based neutron activation and prompt gamma-ray analyses

MATSUE, H., YONEZAWA, C. (JAERI, Tokai)

Multielement determination in new reference materials of sediments prepared at the National Institute of Advanced Industrial Science and Technology of the National Metrology Institute of Japan has been carried out by k_0 -based neutron activation and prompt gamma-ray analyses. The 24 elements such as Na, Cl, K, Ca, Sc, Ti, V, Cr, Mn, Fe, Co, Zn, As, Br, Rb,

Sb, Cs, Ba, La, Ce, Sm, Hf, Ta and Th were determined by the k_0 -NAA. The 15 elements such as H, B, Na, Si, S, Cl, K, Ca, Ti, Cr, Mn, Fe, Cd, Sm and Gd were determined by the k_0 -PGA. Accuracy of the determination was evaluated by analyzing existing reference materials of River Sediment (NIST SRM 1645) and Pond Sediment (NIES No.2).

3P02: Distribution of trace elements at suspended substance-water interface in Lake Biwa

KOJIMA, S., SAITO, T.¹, YOKOTA, K.², FURUKAWA, M.³, TAKADA, J.⁴, ODA, H.⁵, NAKAMURA, T.⁵ (Aichi Med. Univ. School of Med., Radioisotope Res. Center, Osaka Univ.¹, Lake Biwa Res. Inst.², Faculty of Environ. Inform. Sci., Yokkaichi Univ.³, Res. React. Inst., Kyoto Univ.⁴, Nagoya Univ. Center for Chronol. Res.⁵)

Concentrations of trace elements in sediments, pore waters, and suspended substances collected from three sampling sites (23 m depth, 51 m depth and 89 m depth) in the northern basin of Lake Biwa and from one sampling location (4 m depth) in the southern basin of Lake Biwa were determined by instrumental neutron activation analysis (INAA) at Kyoto University Reactor. High concentrations of Al, Mn and Na in suspended substances were observed at surface water in the southern basin of Lake Biwa (4 m depth). Concentrations of Al and Na in suspended substances were much lower between surface water and bottom water at the three sampling sites in the northern basin of Lake Biwa than those in the southern basin of Lake Biwa. Characteristic vertical profiles of concentrations of Mn and Al for the samples of suspended substances collected at the northern basin (89 m depth) on Oct. 30, 1995 were obtained under the condition of thermal stratification.

3P03: Charged particle activation analysis of nitrogen in silicon

Masumoto, K.(KEK), Nozaki, T.(Purex), Yagi, H. (SEI), Minai, Y.(Musashi Univ.), Shikano, K.(NTT), Futatsugawa, S., Saito, Y.(JRIA)

Charged-particle activation analysis (CPAA) has been used for the determination of light elements in various highly purified materials without the effect of its chemical state and the contamination caused by atmosphere. In this work, CPAA was applied to the analysis of trace amount of nitrogen in silicon. Irradiation was performed at Nishina Memorial Cyclotron Center, JRIA. A new irradiation chamber was designed for CPAA. It was confirmed that irradiation and current monitoring were good. Silicon samples were bombarded with 10 MeV proton for 10 min and the $^{14}\text{N}(p, \alpha)^{11}\text{C}$ reaction was used for determination. After irradiation, samples were decomposed with NaOH, oxidized with KMnO_4 . Radioactive carbon was separated as CO_2 and precipitated as lithium carbonate. The annihilation gamma-ray radiated after positron emission from ^{11}C was detected with a couple of BGO-scintillation detectors and a coincidence counting system. We obtained the suitable conditions of irradiation, etching, separation and measurement, in order to recommend the CPAA of nitrogen.

3P04: Photon activation analysis of carbon in glasses used for fiber amplifiers

Shikano, K.(NTT Photonics Labs.), Ohtsuki, T., Yuhki, H.(Lab. Nucl. Sci., Tohoku Univ.), Masumoto, K.(KEK), Mori, A., Shimizu, M.(NTT Photonics Labs.)

We have studied nuclear interference from a matrix produced by (γ, n) , $(\gamma, 2n)$, (γ, p) and (n, γ) reactions and a flow method for ^{11}C separation in order to develop an approach for the photon activation analysis of carbon in InF_3 -based fluoride, chalcogenide and tellurite glasses for fiber amplifiers. We found that seventeen radionuclides are produced from these glasses and chemical separation is necessary to determine carbon. For the flow method, which involves the fusion of an irradiated sample with an oxidizer, the conversion of ^{11}C into $^{11}\text{CO}_2$ and the absorption of ^{11}C in ethanolamine solution, we used a mixture of Pb_3O_4 and B_2O_3 as the oxidizer. We also found that the reaction between $^{19}\text{F}(\gamma, n)$ and $^{23}\text{Na}(\gamma, \alpha n)$ in the ethanolamine solution produced ^{18}F contamination with fluoride and chalcogenide glasses and that this flow method can only be applied to tellurite glasses. We confirmed that the chemical

yield of the flow method was close to 100% when determining carbon in standard steel samples by using lithium carbonate as a standard sample.

3P05: Instrumental neutron activation analysis of extractable organohalogens (EOX) in Weddell seal collected at near Syowa station, Antarctica

Kawano, M.. (Dept. of Environment Conservation, Ehime Univ.), Falandysz, J. (Faculty of Chemistry, University of Gdansk, Poland), Wakimoto, T. (Dept. of Environment Conservation, Ehime Univ.)

Extractable organohalogens (EOX: EOCl, EOBr and EOI) in Weddell seal from the Antarctic marine ecosystem were measured by instrumental neutron activation analysis. The concentration order was EOCl > EOBr > EOI. The concentrations of EOCl were ranged from 16 to 28,000 ng/g on fresh weight basis. On the other hand, DDTs, PCBs and chlordanes compounds (CHLs) were detected as the concentrations in ranging 2.0 to 170 ng/g on fresh weight basis. As shown in the figures, the concentrations of EOCl were relatively high in comparison with the concentrations of DDTs, PCBs and CHLs. This result suggests that the Antarctic animal is contaminated relatively with unknown organochlorine compounds. The bioaccumulation capacities of EOCl and the individual organochlorine compounds were investigated among some samples in different life stage of the animal. The result shows that EOCl is not accumulative in comparison with the known organochlorine compounds such as DDTs, PCBs and CHLs.

3P06: Change of element distribution in rat organs and liver cell fractions under oxidative stress

Endo, K., Ui, I., Matsumoto, K., Yamazaki, M. (Showa Pharmaceutical University)

Contents of iron(Fe), cobalt(Co), zinc(Zn), and Selenium(Se) in the organs (liver, kidney, spleen, heart, lung, and brain) and the liver cell fractions (nuclear, mitochondrial, microsomal, and cytosolic fractions) of Se- or vitamin E(VE)-deficient rats were measured using instrumental neutron activation analysis(INAA). The Fe contents increased mainly in the mitochondrial fraction. Contents of Co in the organs and the liver cell fractions of Se- and VE- deficient rats were markedly low, reflecting the Co contents in the both diets. Contents of Zn in the organs and liver cell fractions of cell fractions of Se- and VE- deficient rats decreased to 60-80% of the contents in normal diets. The Se contents in Se-deficient rat organs except for the kidney, spleen, and brain were below the detectable level under the present conditions. Se-contents in VE-deficient rat decreased to 50-80% of those in normal rats in all organs and fractions. It is suggested that oxidative stress due to Se- or VE-deficiency affects the dynamics of Fe and Zn.

3P07: Variation of elemental composition of airborne dust with environmental condition

Miyamoto, Y., Saito, Y., Magara, M., Sakurai, S., Usuda, S. (JAERI)

For the assessment of environmental impact of radioactive materials and air-pollutants, airborne dust is often used as indicator for the monitoring of these amounts and composition. The dust comes from different origins, and this is direct carrier of these materials. The composition of dust may vary with weather and season. In this work, from the concentration of elements in the dust samples, we tried to clarify the composition of dust and the effect of environmental condition on the composition of dust. The dust samples were collected with a high-volume air sampler at the JAERI. The concentration of elements in the dust samples was determined by instrumental neutron activation analysis. It was found, from the two plots of Sc/Na-Cl/Na ratios and Cl/Al-Sc/Al ratios, that almost all samples consisted of mixture of sea-salt and soil, but some samples consisted of mainly sea-salt. These samples and the sample containing "yellow sand" had same Sc/Al ratio as that of others. But, the sample which was collected at the period when a strong wind blew, the sample had 3 times higher

ratio than that of others.

3P08:Development of a software “Interactive NAA Windows” for neutron activation analysis.

ITO, Y. KAWATE, M. SAWAHATA H., OZAKI, H (Research Center for Nuclear Science and Technology, The University of Tokyo)

A new software on neutron activation analysis is developed for use at the Inter-University Laboratory for the JAERI Facilities. It is Windows-based software written by Visual Basic language. The purpose of the new software is to provide users with self-education of the analysis procedure of NAA. The users can follow every step of the analysis graphically, and this enables them to avoid errors or misjudgments, which are often possible when using sophisticated software. This kind of software is particularly necessary today when NAA has reached maturity and new users tend to neglect fundamental knowledge about the technique.

3P09:Equilibrium charge state measurement of heavy element in He gas using RIKEN gas-filled recoil separator

Kaji, D., Morita, K., Morimoto, K., Y. L. Zhao, H. Xu, Yoneda, A., Suda, T., Yoshida, A., Ideguchi, E., T. Zheng, Ohnishi, T. Haba, H., Katori, K., Sueki, K., Kudo, H., Tanihata, I. (RIKEN, Niigata Univ., Institute of Chinese High Energy Physics, Institute of Chinese Modern Physics, Tsukuba Univ.)

Using a RIKEN gas-filled recoil separator (GARIS) with high intensity heavy ion beams from RILAC, we plan to search for new isotopes, including those of new elements whose atomic number is greater than 113. We need to know the equilibrium charge state, q -bar, of the 113th element in order to make a proper setup of the separator. To estimate the q -bar values of element [113], it is necessary to extrapolate q -bar values of known elements to the new one. Therefore, the performance of the GARIS was studied using recoil atoms with $Z = 84-110$. Measured quantities are equilibrium charge state in helium gas and transmission of the GARIS. Empirical formula was also deduced from these data. In this report, we present the status of heavy element synthesis at RIKEN.

3P10: Basic study of the mass spectrometry using tunable laser

Ishizu, H., Goto, S., Kudo, H. (Fac. of Sci., Niigata Univ.)

Rapid gas phase separations have been applied for the study of chemical properties of trans-actinoid elements. However, the chemical species involved in gas phase chemistry are ambiguous even for their homologs. A mass spectrometry using a tunable laser is examined for the identification of chemical species. In this work, as a basic study for laser ionization, we fabricated an ion detector and examined its performance.

3P11: Isothermal chromatographic behaviors of Ru and Rh volatile complexes

ONO, S., KANEKO, T., GOTO, S., KUDO, H. (Fac. of Sci. Niigata Univ.)

The volatility behaviors of the dipivaloylmethane (dpm) complexes of Ru and Rh isotopes were investigated as a model of their homologues, Hs ($Z = 108$) and Mt ($Z = 109$), using an isothermal chromatography. Ru and Rh isotopes were provided as fission products from ^{252}Cf source, and transported to the reaction chamber using He/KCl gas. The optimum temperature for the reaction between Ru and Rh and dpm was determined to be around 350°C . As the preliminary results, it was found that volatile dpm complexes of Ru and Rh were deposited on the isothermal quartz column under 200°C .

3P12: The estimation of the fast neutron fluence from the Hiroshima atomic bomb by β -ray measurement of ^{63}Ni

Okuda, Y.¹, Ohta, Y.¹, Takamiya, K.², Shibata, S.², Shibata, T.³, Itoh, Y.³, Imamura, M.⁴, Uwamino, Y.⁵, Nogawa, N.⁶, Baba, M.⁷, Iwasaki, S.⁷, Matsuyama, S.⁷ (Grad. School of Eng., Kyoto Univ.¹, Res. Reactor Inst., Kyoto Univ.², Radiation Sci. Center, High Energy Accelerator Res. Org.³, Nat. Mus. of Japanese Hist.⁴, RIKEN⁵, RI Centre, Univ. of Tokyo⁶, Grad. School of Eng., Tohoku Univ.⁷)

In this work, we determined ^{63}Ni (half life 100y) produced in the copper sample by the fast neutrons emitted from the Hiroshima A-bomb ($^{63}\text{Cu}(n,p)^{63}\text{Ni}$). A copper sample (91g) is a lightning rod of San-In Godo Bank (850m slant range). Ni was chemically separated from the copper sample, and ^{63}Ni was measured by liquid scintillation counter at RI Centre, Univ. of Tokyo. Corrections of chemical yield, quenching effect and ^{63}Ni produced by $^{62}\text{Ni}(n_{th}, \gamma)^{63}\text{Ni}$ were carried out, and ^{63}Ni by fast neutrons was determined to be 8.04×10^5 atom/gCu.

3P13:Electronic structures of fluoride complexes of rutherfordium and the 4th row elements

HIRAI,T.(Niigata Univ.), HIRATA,M., NAGAME,Y.(JAERI), KUDO,H.(Niigata Univ.)

Many experiments in gas and liquid phase to study chemical properties of Rf were carried out. In ion exchange chromatography experiments with hydro fluoric acid, some interesting results are obtained, but chemical species in that solution are in study. In this work, we calculated the electronic structure of fluoride complexes of Rf and other 4th row elements with the discrete-variational X α (DV-X α) method. Energy level schemes of ZrF $_7^{3-}$, HfF $_7^{3-}$, and RfF $_7^{3-}$ were similar and each surface charge density of them are not so different. In the experimental study of the ion-exchange chromatography, behavior of Zr and Hf was similar, but Rf was quite different. Thus it is suggested that Rf does not form the heptafluoride complex in the condition for the chromatography. Since effective charges of F decreased with increasing distances between Rf and F. This indicates that bond nature of them is ionic one.

3P14:Anomalous excitation energy dependence of shell effects in asymmetric actinide fission

Nishinaka, I.(Advanced Science Res. Center, Japan Atomic Energy Res. Institute), Tanikawa, M.(School of Science, Univ. of Tokyo), Goto, S.(Department of Chemistry, Niigata Univ.), Nagame, Y., Nishio, K.(Advanced Science Res. Center, Japan Atomic Energy Res. Institute), Yokoyama, A.(Department of Chemistry, Kanazawa Univ.), Asai, M.(Advanced Science Res. Center, Japan Atomic Energy Res. Institute), Haba, H.(Cyclotron Center, RIKEN), Ichikawa, S., Tsukada, K., Akiyama, K.(Advanced Science Res. Center, Japan Atomic Energy Res. Institute), Toyoshima, A.(Department of Chemistry, Osaka Univ.), Kudo, H.(Department of Chemistry, Niigata Univ.)

Fission fragment pairs were measured in coincidence by a double time-of-flight method in the fission of p + ^{232}Th at incident beam energies of 10.0, 11.5, and 13.0 MeV. With increasing incident proton energy, the relative mass yields at A = 143 decreased rapidly compared with those at A = 132 in the asymmetric fission mode. The fragments with A = 143 and A = 132 correspond to the deformed shell of N = 86-88 and the spherical shells of Z = 50 and N = 82, respectively. In contrast to general dependence of shell effects on excitation energy, increasing excitation energy influences adversely the shell effects of N = 86-88 compared with those of Z = 50 and N = 82. Hence it is found that experimentally observed excitation energy dependence of mass yields is anomalous in view of fragment shell effects.

3P15:Systematic study of asymmetric mass division in proton-induced fission of actinides

Goto, S., Kaji, D., Kudo, H. (Fac. of Sci., Niigata University), Nishinaka, I., Nagame, Y., Ichikawa, S., Tsukada, K., Asai, M. (JAERI), Haba, H. (RIKEN), Tanikawa, M. (Fac. of Sci., The University of Tokyo)

In order to study the correlation between the asymmetric mass distribution and the shell structure of fission fragments, the fragment mass and energy distributions in the proton-induced fission of ^{232}Th , $^{233,235,238}\text{U}$, ^{237}Np , and $^{239,242,244}\text{Pu}$ were precisely measured using a double time-of-flight method. The obtained mass distributions of the fission fragments were decomposed to two components, symmetric and asymmetric fission components, by the two-component analysis of the total kinetic energy distribution of the fission fragments. It was found that the light side of the heavy fragment mass distribution shifted to heavier mass number with the increase of neutron-to-proton ratios of the fissioning nuclei. The results are explained by a fragment shell of $Z=50$.

3P16:Radiochemical yield measurement on the fragmentation products from ^{197}Au target with high-energy ^{12}C ions by radiochemical separation

Murae, T., Kikunaga, H., Kinoshita, N., Yokoyama, A. (Faculty of Science and Graduate School of Natural Science and Technology, Kanazawa Univ.) Ohki, T., Shigekawa, M., Kasamatsu, Y., Shinohara, A. (Graduate School of Science, Osaka Univ.) Shibata, S. (National Institute of Radiological Sciences) Saito, T. (Radioisotope Res. Center, Osaka Univ.)

Our group had been engaged in a series of experiments on target fragmentation of $^{\text{nat}}\text{Cu}$, ^{93}Nb , ^{141}Pr , ^{197}Au nuclei etc. using high-energy heavy ions of ^{12}C (180-400 MeV/u), ^{28}Si (290-800 MeV/u), and ^{40}Ar (290-650 MeV/u) from HIMAC (Heavy Ion Medical Accelerator in Chiba) of the National Institute of Radiological Sciences, Japan. Yield measurement of the fragmentation products from ^{197}Au bombarded with 400 MeV/u ^{12}C ions were nondestructively assayed by gamma-ray spectrometry in a previous study. In the present study, we obtained additional data for the same system by using gamma-ray spectrometry combined with chemical separation for the elements of Ni, Sr, Y, Zr, Nb, Ag, Cs, Ba, rare earths (group separations), Hf, Ta, Re, Os, Ir, Pt and Au. Isobaric yields for this system were deduced from the measured cumulative yields of nuclides together with the previous nondestructive data and compared to the EPAX II calculation.

3P17:The estimation of the fast neutron fluence from the Hiroshima atomic bomb by β -ray measurement of ^{63}Ni

Okuda, Y.¹, Ohta, Y.¹, Takamiya, K.², Shibata, S.², Shibata, T.³, Itoh, Y.³, Imamura, M.⁴, Uwamino, Y.⁵, Nogawa, N.⁶, Baba, M.⁷, Iwasaki, S.⁷, Matsuyama, S.⁷ (Grad. School of Eng., Kyoto Univ.¹, Res. Reactor Inst., Kyoto Univ.², Radiation Sci. Center, High Energy Accelerator Res. Org.³, Nat. Mus. of Japanese Hist.⁴, RIKEN⁵, RI Centre, Univ. of Tokyo⁶, Grad. School of Eng., Tohoku Univ.⁷)

In this work, we determined ^{63}Ni (half life 100y) produced in the copper sample by the fast neutrons emitted from the Hiroshima A-bomb ($^{63}\text{Cu}(n,p)^{63}\text{Ni}$). A copper sample (91g) is a lightning rod of San-In Godo Bank (850m slant range). Ni was chemically separated from the copper sample, and ^{63}Ni was measured by liquid scintillation counter at RI Centre, Univ. of Tokyo. Corrections of chemical yield, quenching effect and ^{63}Ni produced by $^{62}\text{Ni}(n_{\text{th}}, \gamma)^{63}\text{Ni}$ were carried out, and ^{63}Ni by fast neutrons was determined to be 8.04×10^5 atom/gCu.

3P18:Measurement of half life of ^{53}Mn (III)

Oura, Y., Nagamine, T., Ebihara, M., Yoneda, S., Honda, M. (Graduate School of Sci., Tokyo Metropolitan Univ., National Sci. Museum, Nihon Univ.)

The half life of ^{53}Mn was measured with using ^{53}Mn extracted from iron meteorite, ALH77250. The value of half life was calculated from activity and number of atoms of ^{53}Mn because of its long life. Activity of ^{53}Mn was determined by measuring characteristic X ray accompanied with EC decay and the number of atoms of ^{53}Mn was obtained from both of

the amount of Mn determined by INAA and $^{53}\text{Mn}/^{55}\text{Mn}$ atomic ratio by thermal ionization mass spectrometry. Finally we obtained $(3.0 \pm 0.1) \times 10^6$ years of half life of ^{53}Mn . This value are 20% shorter and has higher precise than one cited in Table of Isotopes .

3P19:Reinvestigation of the half-life of samarium-147

Kinoshita, N., Nakanishi, T.¹, Yokoyama, A.¹. (Graduate School of Natural Science and Technology, Kanazawa Univ., Department of Chemistry, Faculty of Science, Kanazawa Univ.¹.)

Samarium-147 is a naturally occurring long-lived alpha emitter. The half-life value currently adopted for this nuclide was determined in 1970 to be $(1.06 \pm 0.02) \times 10^{11}$ y, but the half-life of ^{147}Sm has not been reevaluated since 1971. Thus, the half-life of ^{147}Sm is reevaluated using current techniques. In the present work, counting sources were prepared as follows: known amounts of ^{147}Sm and alpha emitter standard (^{210}Po , ^{238}U , or ^{241}Am) were mixed well and evaporated on a watch glass. Alpha spectrometry was carried out using Si surface barrier detector. Alternatively, known amounts of ^{147}Sm and alpha emitter standard (^{241}Am) were dissolved in liquid scintillation cocktail to measure by using liquid scintillation counter. Alpha disintegration rate of known amounts of ^{147}Sm was thus determined referring to alpha activity of alpha emitter standard, and the half-life of ^{147}Sm was calculated. The half-life value obtained in this work is $(1.17 \pm 0.02) \times 10^{11}$ y.

3P20:Hydrolysis Reactions of Thorium(IV) Aqua Ion, as Studied by Quantum Chemistry Methods

Yang, T.X., Tsushima, S., Suzuki, A. (Dept. Quantum Engineering and Systems Science, Univ. of Tokyo)

Hydration number of $\text{Th}(\text{OH})_4(\text{H}_2\text{O})_n^0$ cluster and the hydrolysis of reactions of Th^{4+} aqua ion were studied using quantum chemistry methods. The calculations are based on HF/6-31G* level of theory. The effects of solvent were calculated by including the second hydration shell explicitly. The results show that the primary hydration number of $\text{Th}(\text{OH})_4(\text{H}_2\text{O})_n^0$ cluster is 8. The hydrolysis species and hydrolysis reactions of Th^{4+} aqua ion based on $\text{Th}(\text{H}_2\text{O})_9(\text{H}_2\text{O})_{18}^{4+}$ were calculated.

3P21:Luminescence and IR studies on structural determination of extracted complexes of lanthanides(III) and curium(III) with Cyanex301, Cyanex302 and Cyanex272

Guoxin, T.; Kimura, T.; Yoshida Z., Kato Y. (Advanced Science Research Center, JAERI)

Cyanex extractants (Cyanex301, 302 and 272), i.e., three kinds of organophosphorous acids with same substitutive alkyl structure and different function groups, have quite different extraction properties for trivalent lanthanides (Ln) and actinides (An). Cyanex301 has excellent selectivity for An(III) over Ln(III) relative to the poor selectivity of Cyanex302 and 272. The structure of extracted complexes of Ln(III) (Ln = Sm, Eu, Tb, Dy) and Cm(III) with Cyanex301, 302 and 272 was investigated using Time Resolved Laser-induced Fluorescence Spectroscopy (TRLFS) and FT-IR spectroscopy. The results of luminescence and IR measurements indicate that there are 1 or 2 H_2O coordinated to Ln(III) but no H_2O coordinated to Cm(III) in the extracted complexes with Cyanex301. There are 3 to 5 H_2O in the first coordination shell of Ln(III) and Cm(III) in the complexes with Cyanex302, and the deduced molecular formula is $\text{ML}_3 \cdot n\text{H}_2\text{O}$. There is no H_2O in the first coordination shell of Ln(III) and Cm(III) in the extracted complexes with Cyanex272.

3P22:Determination of Gibbs energy for ion transfer of actinides between aqueous and organic solution phases by radio-voltammetry at liquid-liquid interface

KITATSUJI, Y.¹, KIMURA, T.¹, KUDO, H.², KIHARA, S.³, YOSHIDA, Z.¹ (1 Japan Atomic

Energy Res. Inst., 2 Graduate School of Sci., Tohoku Univ., 3 Dep. of Chemistry, Kyoto Inst. of Technol.)

Radio-voltammetry at the interface between two immiscible electrolyte solutions phases (ITIES) has been developed based on the controlled-potential electrolysis and the radiometric determination of concentration of the ion in both phases. Relationship between the electrolysis potential and distribution ratio of the ion (D) is measured after ion transfer equilibrium is attained. Transfer of Am^{3+} between aqueous and nitrobenzene solutions was investigated by radio-voltammetry. The plot of the electrolysis potential and the logarithmic distribution ratio of Am^{3+} showed linearity at the potential range of more negative than +0.33 V vs TPhE. The slope of the line was +0.021 V / log D , which shows that the log D vs E_{CPE} plot is expressed by Nernst equation. Standard potential and standard Gibbs energy for the transfer of Am^{3+} between aqueous and nitrobenzene phases were determined to be +0.390 V and 113 kJ mol⁻¹, respectively.

3P23: Increases of environmental gamma-ray dose originated from winter thunderstorms.

Yamazaki, K., Tonouchi, S., Tanabe, H. (Niigata Pref. Inst. Env. Rad. Mon.), Hashimoto, T. (Niigata Univ.)

Cumulative dose measurements have been performed at the points from 1m to 117m above the ground on the arrester tower located at the site of the Kashiwazaki Kariwa nuclear power station using radiophotoluminescence glass dosimeter (RPLD) and thermoluminescence dosimeter (TLD).

From the measurement results, the mean dose rates both from RPLD and TLD gradually decrease with height in summer season. On the other hand, the vertical profile of upper regions showed in the reverse attenuation in winter season. It was assumed that the increasing trend of dose rates with height is caused by some external radiation source peculiar to winter season.

In this winter, many thunderstorms occurred and dose rates from both NaI(Tl) and IC detectors increased occasionally at monitoring stations.

According to the Monte Carlo calculation of the behaviour of electrons and photons in the model thundercloud, it was suggested that bremsstrahlung X-rays generated at high altitude has been attributed to the radiation source.

3P24: Seasonal variation of atmospheric concentrations of ²¹⁰Pb and ⁷Be at Sarufutsu, Hokkaido

Sato, S., Koike, Y.¹, Saito, T.¹, Sato, J.¹ (Sarufutsu Takushin Jun. High School, School of Sci. and Technol., Meiji Univ.¹)

Atmospheric concentrations of ²¹⁰Pb and ⁷Be were observed at Sarufutsu on the coast of the Sea of Okhotsk in the northern part of Hokkaido, Japan. Observations were carried out during the period from Feb., 2001 to Mar., 2002. The atmospheric concentrations of ²¹⁰Pb and ⁷Be ranged from 0.2 to 2.7 mBq/m³ and from 0.0 to 5.3 mBq/m³, respectively.

The atmospheric ²¹⁰Pb concentration showed a "one-peak" variation pattern which was similar to that observed at the eastern part of the Chinese Continent; the maximum levels were recorded in winter season. The high concentrations of atmospheric ²¹⁰Pb observed in winter season may be due to the atmosphere from the Chinese Continent. Though the seasonal variation of atmospheric concentration of ⁷Be was similar to that of ²¹⁰Pb, no significant correlation between the atmospheric concentrations of ²¹⁰Pb and ⁷Be was obtained at Sarufutsu.

3P25: Estimation of regional change of atmospheric ¹⁴C in Japan based on rice grain ¹⁴C contents.

Shibata, S. Kawano, E. (Radiation Res. Center, Osaka Prefecture University)

We collected rice grains on a nationwide scale every three years for 17 years from 1982 to 1999. We have measured their ^{14}C contents for estimating the atmospheric ^{14}C contents of Japan. The atmospheric ^{14}C contents show no correlation with the latitudes of their locations. There is a small correlation opposite to the population densities of their locations. The atmospheric ^{14}C contents of Japan keep gradually decreasing and show slightly higher values ($81.4 \pm 11.1\%$) than nature at the summer in 1999. Two graphs are shown. One of the graphs shows the relation between the rice grain ^{14}C contents and their location's latitudes. The other graph shows the variation of the atmospheric ^{14}C contents of Japan for 17 years from 1982 to 1999.

3P26: Measurement of rhenium in water-soluble fraction of soils

Tagami, K., Uchida, S. (Environ. Toxicol. Sci. Res. Group, Natl. Inst. Radiol. Sci.), Twining, J. (Environ. Div., Australian Nucl. Sci. Tech. Organisation)

To understand Tc-99 behavior in soil systems, we have measured Re as a chemical analogue of Tc for their physico-chemical similarities. Soil samples, Tippera and Blain, were collected in Northern Territory, Australia. Total and water soluble Re concentrations were measured using 2-g and 50-g samples, respectively. Rhenium was chemically separated before ICP-MS measurement. The results showed that total Re contents in Tippera were about 5 times higher than those in Blain. The percentages of water soluble Re depended on soil type, e.g., $3.6 \pm 2.3\%$ for Tippera and $12 \pm 10\%$ for Blain for the samples collected in 2000. The dynamic equilibrium between water soluble and non-water soluble Re has been reached over geological time periods, therefore, the relatively low water soluble fractions in these soils is not unexpected, particularly as the Re originates from the mineral matrix. Because the water soluble fraction plays an important role for the in root uptake by plants, Re transfer from the soil to plants would be affected by this condition.

3P27: Accumulation of radionuclides in sediment

Kanai, Y. (Geological Survey of Japan, AIST)

Inventories of Pb-210ex and Cs-137 in sediments taken from Lake Suwa, Lake Shinji, Lake Nakaumi, the Sea of Japan, Chinese lakes and Nepal lakes were studied. Both inventories are in good correlation with each other, and the ratio varied with the station. In order to elucidate the state of radionuclides in sediment, chemical leaching technique was applied to the lake sediments (Lake Shinji). Most of Pb-210 and Cs-137 were present in silicate fraction (probably in clay minerals). A part of Pb-210ex was present in Fe-Mn oxide fraction and for coarser grains also in carbonate fraction. The reason is supposed to be that the supply of Pb-210 is larger in ocean and the adsorption of Cs-137 is affected by co-existing cations.

3P28: An application of hollow-fiber polyimide membrane to continuous tritium monitoring systems

Tega, E., Shimada, A., Kimura, H., Oyaidu, M., Sasaki, M., Kodama, H., Morimoto, Y., Okuno, K., Sasaki, S.¹, Suzuki, T.¹, Kondo, K.¹ (Radiochemistry Res. Lab., Fac. of Sci., Shizuoka Univ., KEK¹)

In high-energy accelerator facilities, various kinds of airborne radionuclides such as ^3H , ^{11}C , ^{13}N , ^{15}O and ^{41}Ar are produced in the accelerator beam-line tunnel through nuclear spallation reactions of primary/secondary particles with air elements during machine operation. In order to attain the direct and continuous monitoring of tritium in the air released from the facility, it is essential to separate tritium from the other radionuclides. We have been developing the method to separate and enrich tritium with a hollow-fiber polyimide membrane. In this present study, we investigated the separation characteristic of water vapor from air

using a small membrane module.

3P29: Radioiodine absorption by activated carbon fibers

Nogawa, N. , Arai, Y. , Okuda, A. , Makide, Y. (Radioisotope Center, The university of Tokyo), Wakaida, Y. (Wakaida Engineering Inc.)

Granulated active carbons have been widely used for the collection of radioiodine in the air. Activated carbon fibers (ACFs) large by produced in the factory were examined on the collection and retention capacity for iodine compounds comparing with granulated active carbons.

The collection efficiencies of the felt and knit form ACFs were better than those of granulated active carbons for gaseous inorganic iodine. Collection efficiency was lowered with the increases of iodine concentration and air speed.

The relationship between the loaded quantity of triethylendiamine (TEDA) and the retention capacity (weight per unit weight) of felt ACF for methyl iodide was 0 % : 0, 2 % : 0.18 and 4 % : 0.23 respectively after 9 days left open in the air.

3P30: Investigation on the *black rain* from the Hiroshima A-bomb – Metal element analysis of sediment core samples from Mitaki, Hiroshima

Fujikawa, Y. (Research Reactor Institute, Kyoto Univ.), Shizuma, K., Endo, A. (Grad. School of Eng., Hiroshima Univ.), Ikeda, E. (Kankyo Gijyutu Co.), Fukui, M. (Research Reactor Institute, Kyoto Univ.)

In our previous study, we detected excess ^{137}Cs , Pb and Zn, and anomalous $^{235}\text{U}/^{238}\text{U}$ ratios from the plastered wall with streaks of *black rain* from Hiroshima A-bomb. In order to clarify the fate of these elements that was deposited with the rain, we collected and analyzed sediment samples from Nissyoen, Mitaki, Hiroshima where the *black rain* fell after the detonation. Depth profiles of metal elements in the sediment showed higher concentrations of Pb and Zn in the top-layer. U and Pb isotope ratio analyses is now under way to clarify the origin of excess metal elements in the samples.

3P31: Mutual separation of Eu and Ac for the determination of ultra low-level radioactivity of ^{152}Eu in samples exposed to atomic bomb

Izumi, H., Nakanishi, T.¹ (Department of Chemical Science, Graduated School of Natural Science and Technology, Kanazawa University, ¹Department of Chemistry, Faculty of Science, Kanazawa University)

For the determination of ultra low-level radioactivity of ^{152}Eu in samples exposed to atomic bomb, lanthanoide-enriched fraction was chemically separated from concrete samples exposed to the Nagasaki a-bomb, and gamma-spectrometry was carried out, but ^{152}Eu determination was seriously interfered with ^{227}Ac . Thus, mutual separation of Eu and Ac with di(2-ethylhexyl)phosphoric acid (HDEHP) was studied. After extraction of Eu and Ac from 0.1 mol/L HNO_3 into organic phase, washing procedures using 0.2 mol/L HNO_3 were repeated for the organic phase to remove Ac. As a result of tracer experiments, we found a possibility of mutual separation of Eu and Ac.

3P32: Measurement of Ra-226 in environmental water by liquid scintillation counting

HEYUAN, Z. (Grad. Sch. Sci. Tech., Kumamoto Univ.), MOMOSHIMA, N. (Fac. Sc. Kumamoto Univ.)

A modified simple method that uses an α/β separation liquid scintillation counter (LSC) is developed for determination of ^{226}Ra concentration in environmental water samples. ^{226}Ra in water is coprecipitated in BaSO_4 . The precipitate is dissolved with EDTA4Na solution and kept in a glass gas-bubbler until ^{222}Rn grows. We used ^{222}Rn -emanation procedure to measure

^{226}Ra . The ^{222}Rn emanated by bubbling of N_2 is collected in a Tetra bag and then introduced to an U tube, in which glass debris was filled and cooled at liquid nitrogen temperature. After washing the U tube with scintillator, the scintillator and the glass debris were transferred to a 20 ml counting vial. ^{222}Rn and daughter nuclides were measured with the α/β LSC. The α counts were extracted from a 3-dimensional graph, which consists of particle energy, α and β pulse level index, and counts

3P33:U-234/U-234 activity ratio in water brought into contact with rock

Yamada, Y., Nakanishi, T.¹, Hama, K.² (Graduate School of Natural Sci. and Technol., Kanazawa Univ., ¹Fac. of Sci., Kanazawa Univ., ²JNC)

Groundwater plays an important role in transport of materials in underground geological media, and in order to introduce a time scale into the groundwater system various dating methods of groundwater have been studied. In this work radioactive disequilibrium between U-238 and U-234 (U-234/U-238 activity ratio > 1) was studied for the dating of groundwater, and the results of leaching experiments showed that U-234/U-238 activity ratio of uranium leached out of fresh rock with distilled water goes up to ~ 3.2 . This result and analytical data for groundwater and rock from a drilling site of JNC was applied to a model equation for U-234/U-238 dating.

3P34:ICP-MS analysis of river water around former uranium mine in Uzbekistan

KO, S.(Graduate School of Agr., Kyoto Univ.), AOKI, T.(Radioisotope Res. Center, Kyoto Univ.), KATAYAMA, Y.(Univ. of Human and Environment)

Uranium production of Uzbekistan is ranked 5th in the world. Yangiabad uranium mine, in the Fergana valley was in operation until 1960s. After that, dumps have been left without sufficient measures. Outflow from the former mine is used for irrigation in the highly populated area, exposing the adjacent environment and inhabitants in danger by chemical and radioactive harmful substances. In this study, water quality of the river in the region was analyzed for preliminary understanding of present condition. Concentration of major ions and trace elements in the water samples taken from Akhangaran river basin around Yangiabad was analyzed by ion chromatography and ICP-MS. It should be noted that the concentration of uranium in most of the samples exceeded the standard of WHO guideline. It is suggested that plants, animals and people in the region are in danger if the dumps are left in the current situation, although people do not drink the river water directly. Further monitoring is required for safety management.

3P35:The sinking behavior of Pu-239,240 in open-ocean water column (the Izu-Ogasawara and Japan Trenches)

Nishizawa, A., Nakanishi, T.¹. (Graduate School of Natural Science and Technology, Kanazawa Univ., Department of Chemistry, Faculty of Science, Kanazawa Univ.¹.)

The 1984 and 1994 depth distributions of $^{239,240}\text{Pu}$ in water columns and 1994 inventory of the nuclides in surface sediments of the Izu-Ogasawara and Japan trenches have been measured to discuss open-ocean sinking behaviour of fallout Pu. The Pu concentrations were detectable throughout the water columns from the surface to the bottom depths (~ 10 km). It was found that considerable change took place during 1984 and 1994 in the vertical profile and water-column inventory of Pu: at Izu-Ogasawara Trench the Pu inventory in water column from 2 km deep to 10 km deep layer increased from 2.8 mBq/cm² (in 1984) to 7.4 mBq/cm² (in 1994). This may be explained by the lateral transport of Pu from Pacific Basin to Izu-Ogasawara Trench at the water layer deeper than 5 km.

3P36:Measurements of natural neutron around UTR-KINKI by activation of gold

¹MURATA, Y., ¹KOMURA, K., ¹AHMED, M. Y., ¹SUZUKI, A., ²KOGA, T., ²MORISHIMA, H.
(¹LLRL, Kanazawa Univ., ²Atomic Energy Research Institute, Kinki Univ.)

Some pure gold plate (ca. 7 g) and gold grain (ca. 20 g) were set around the University Training and Research Reactor of Kinki University to investigate the availability of gold as detector of neutron flux of the order of $10^{-2} \sim 10 \text{ n}\cdot\text{cm}^{-2}\cdot\text{s}^{-1}$. The gold samples were set at 3 ~ 320 m from the reactor core, and exposed for 2 ~ 30 days. ¹⁹⁸Au, generated by neutron capture reaction in the gold samples, was measured by using ultra low background Ge detectors installed in Ogoya underground laboratory (270 m water equivalent). The atom number of ¹⁹⁸Au in the gold samples was measured to be ranging from 50 to 1000 g⁻¹-Au. Counts of neutron using ³He neutron counter showed good agreement with the atom number of ¹⁹⁸Au. This result indicates that gold can be used as a standard detector for neutron flux of $\sim 10^{-3} \text{ n}\cdot\text{cm}^{-2}\cdot\text{s}^{-1}$ under severe environmental conditions without the electricity.

3P37: Further investigation on radioisotopic impurities in bismuth chemicals

SAITO, T., YAMAGUCHI, Y., KOJIMA, S.¹ (Radioisotope Res. Center, Osaka Univ., Nucl. Med. Center, Aichi Med. Univ.¹)

We have already established that various bismuth chemicals contain trace amounts of radioisotopic impurity, ²⁰⁷Bi. Recently we have re-measured these samples with a new well-Ge spectrometer. The atom ratio of ²⁰⁸Bi to ²⁰⁷Bi is confirmed to be approximately 1000, which is apparently inconsistent with those obtained at Eniwetak and Bikini test sites. This fact indicates that the radioisotopic impurities in bismuth chemicals possibly originate in nuclear test explosions other than the US tests held at the above sites.

3P38: AMS radiocarbon dating of the fragments from ancient Japanese calligraphies

Oda, H., Nakamura, T. (Center for Chronological Res., Nagoya Univ.), Ikeda, K. (Faculty of Literature, Chuo Univ.)

It was indicated by the previous work on radiocarbon dating ancient Japanese documents of known age that Japanese paper is a suitable sample for radiocarbon dating, because of small discrepancy between the calibrated radiocarbon age and the historical age. In this study, we measured radiocarbon ages of the paper fragments from ancient Japanese calligraphies of unknown age by AMS. Although these calligraphies are attributed to the poets who were active in Heian or Kamakura period (roughly corresponds to the 11th or 12th century), paleographical studies suggested that they were written in the later period. This suggestion was supported by radiocarbon ages that ranged from 17th to 20th century. There are many counterfeit or copied fragments among the calligraphies attributed to the famous poets. This study showed that radiocarbon dating gives an answer for the argument about the authenticity of calligraphy.

3P39: Current status of ³⁶Cl-AMS at MALT.

AZE, T. (Graduate School of Integrated Basic Sciences, Nihon University), FUJIMURA, M. (College of Humanities and sciences, Nihon University), NOGUCHI, M. (College of Humanities and sciences, Nihon University), MATSUMURA, H. (High Energy Accelerator Research Organization), NAGAI, H. (College of Humanities and sciences, Nihon University), MATSUZAKI, H. (Research Center for Nuclear Science and technology, The University of Tokyo)

We report the current status of ³⁶Cl-AMS at MALT (Micro Analysis Laboratory, Tandem Accelerator), The University of Tokyo. Since the maximum acceleration voltage of the tandem accelerator of MALT is 5 MV, energy of the accelerated ³⁶Cl ions is not high enough to identify the isobar ³⁶S. Therefore, we used the GFM (gas filled magnet) to separate ³⁶Cl and ³⁶S. GFM can separate the ³⁶Cl and ³⁶S ions spatially, and the ³⁶S has decreased by 1/1000. By measuring the energy loss and the residual energy of the ions in the ³⁶Cl region with a gas

counter, the interference of ^{36}S ion has decreased further. The reproducibility in the replicated measurements was about 10% and the sensitivity for $^{36}\text{Cl}/\text{Cl}$ ratio was about 10^{-10} .

3P40: The present status of ^{36}Cl measurement by Accelerator Mass Spectrometry in the University of Tsukuba

Matsuhiro, T., Seki, R., Nagashima, Y., Takahashi, T. (AMS group of the University of Tsukuba)

The ^{36}Cl element has been measured with an accelerator mass spectrometry system (AMS) at the University of Tsukuba. The ^{36}Cl is a long half-life radio-nuclide, $T_{1/2} = 3.01 \times 10^5$ years, and its natural existence is a very little. As ratios of ^{36}Cl to ^{35}Cl of environmental samples are from 10^{-15} to 10^{-12} , direct measurement of radiation is very difficult. Nowadays we obtained the lowest limit of detection is the ratio $^{36}\text{Cl}/^{35}\text{Cl} = 1 \times 10^{-14}$. We have performed re-evaluation of the Dosimetry System 1986 by ^{36}Cl in Hiroshima granite. Further we will measure ^{36}Cl in soils from the surroundings of nuclear reactors and in the shielding concrete of accelerators. To obtain more precision of measurement, the modifications of AMS system, for example raising the stabilization of 12UD Pelletron tandem and elimination of S, are in progress.

3P41: Measurement of the rate constants between polyphenols and the hydroxyl radical - comparison of a new rapid flow-ESR and the ESR spin trapping methods

Ohashi, Y., Tsuchiya, H., Yoshioka, H., Yoshioka, H. (Radiochem. Res. Lab., Fac. of Sci., Shizuoka Univ.; Inst. for Environ. Sci., Univ. of Shizuoka)

A new method using rapid flow-ESR was proposed for measuring rate constants of PPs with hydroxyl radical (HO). An ER4117D-MVT dielectric mixing resonator (DMR, Bruker) was used for the detection of polyphenol (PP) radical with short lifetime produced by the reaction with the HO. The solution A (0.01 M TiCl_3 + PP + 0.25 M EtOH + 0.2 M H_2SO_4) and the solution B (0.09 M H_2O_2 + 0.2 M H_2SO_4) flowed at a constant rate and mixed in the DMR. EtOH was used as a standard. ESR signals of PP and 1-hydroxyethyl radicals generated by the reaction with HO were detected simultaneously, and the ratio of rate constants of PP and EtOH was calculated from the ESR intensities of these radicals. As well deviation was observed when the ratio was calculated only from the intensity change of the 1-hydroxymethyl radical; some approximation being used in the spin trapping method.

3P42: Site specificity of DNA scission by ^{60}Co gamma-ray irradiation - DNA secondary structures specific scission-

Sakamoto, F., Narumi, I.¹, Uchida, S.². (JAERI Tokai, JAERI Takasaki¹, Tokyo Nuclear Service²)

Form I type of pBR322 plasmid DNA was cleaved by ^{60}Co gamma-ray irradiation. The DNA scission sites were determined by a novel method we devised. We researched the relationship between the scission sites and the kinds of base, the base sequences and the secondary structures of DNA. In order to the research, we simulated the secondary structures of the DNA by using a program to estimate RNA secondary structure. As a result, though it seems that the scission sites are not influenced both by kinds of base and by base sequences, the scission sites have possibly relevance to the secondary structure of the DNA. Most of scission sites are located on the loop positions of the secondary structures. The steric structures of the DNA are being now simulated

3P43: Development of the production and separation of KUR multitracer

Nakamura, M.¹, Takamiya, K.², Shibata, S.², (Grad. School of Eng.¹, Kyoto Univ., Res. Reactor Inst., Kyoto Univ.²)

KUR multitracer includes radioactive isotopes produced by thermal neutron fission of ^{235}U . In this work, we have developed the mutual separation method of these isotopes included in the KUR multitracer solution using ion exchange method. In comparison with solvent extraction method, additional agents such as complexing reagent and/or buffer solution are unnecessary in this method. In this work, Dowex1-X8 was used as anion exchange resin in order to investigate the adsorption and desorption of the radioactive isotopes in various concentration of HCl and HNO_3 . Finally, suitable condition for separating ^{239}Np , ^{95}Zr , ^{103}Ru , lanthanoid elements and ^{140}Ba was determined. A scheme of mutual separation of KUR multitracer was constructed.

3P44:Radiochemical study on the local distribution of zinc in brain

Tarohda, T. (Graduate School of Natural Science and Technology, Kanazawa Univ.)
Yabushita, Y., Amano, R. (School of Health Science, Faculty of Medicine, Kanazawa Univ.)

Stable Zn distribution and ^{65}Zn uptake in the brains of mice fed zinc controlled diet were evaluated during development using Timm stain and autoradiography, respectively. Hippocampal mossy fiber was imaged with both Timm stain and ^{65}Zn autoradiography. ^{65}Zn autoradiography has been shown to trace zinc uptake behavior in hippocampal mossy fiber of developmental mice. Mossy fiber sprouting was normally observed in the hippocampus of zinc-deficient mice, although hippocampal mossy fiber of mice fed zinc-deficient diet was smaller in size than that of mice fed normal diet. On the other hand, ^{65}Zn uptakes in thalamus and hypothalamus were found to be high with autoradiography, although stable zinc distribution was observed to be low with Timm stain. On the contrary, in amygdala Zn distribution was observed to be high. These results suggest that the difference of Zn distribution and ^{65}Zn uptake among various brain regions was related to the chemical state of Zn, inorganic Zn or protein-bound Zn. Therefore, it is very useful to compare the ^{65}Zn autoradiography with Timm stain for understanding Zn biobehavior.

3P45:Labeling of bifunctional chelating agents with ^{188}Re for radiotherapy

Hashimoto, K., Matsuoka, H. (Dep. of Res. Reactor, Japan Atomic Energy Res. Inst.), Uchida, S. (Tokyo Nuclear Service, Co.)

The labeling of useful bifunctional chelating agents for radiotherapy (TETA, DOTA and MAG_3) with generator-produced ^{188}Re was investigated in detail. TETA and DOTA have N_4 donor atoms and MAG_3 has N_3S donor atoms. The dependence of the labeling yield upon the reaction conditions such as the concentrations of the reducing agent and the ligand, pH, temperature and the addition of a carrier was examined. Under the optimum conditions, the labeling yield of ^{188}Re -TETA was 80% using carrier-added ^{188}Re and 60% using no-carrier-added ^{188}Re . However, the ^{188}Re -TETA was not stable even in the reaction mixture. Furthermore, the reaction conditions for the labeling of DOTA and MAG_3 , and their stability were studied.

3P46:Multitracer screening for RI delivery manner — Brain rubidium uptake bypassing blood-brain-barrier —

Kanayama, Y., Enomoto, S*, Amano, R. (School of Health Sciences, Faculty of Medicine, Kanazawa University., *The Institute of Physical and Chemical Research (RIKEN).)

Brain metal uptake is closely associated with metal delivery manner. The multitracer (MT) technique was applied to learn the differences of brain uptake and elimination of trace elements among 8 different administration methods. The physiological MT solution was administered in 8 different methods (intravenous, intraperitoneal, intranasal (IN), intramuscular, subcutaneous, intracutaneous, percutaneous, and peroral administration) into ICR mice. The brain, blood and plasma were obtained at plural time intervals within 24

hours after administration. As a result, the simultaneous tracing of ^7Be , ^{46}Sc , ^{48}V , ^{51}Cr , ^{54}Mn , ^{59}Fe , ^{56}Co , ^{65}Zn , ^{74}As , ^{75}Se , ^{83}Rb , ^{85}Sr , ^{88}Y , ^{88}Zr , $^{95\text{m}}\text{Tc}$ and ^{103}Ru were observed. The brain and blood uptake of Rb were increasing with time, but the plasma uptake of Rb were decreasing in all methods. In addition, the brain uptake rates of Rb by IN was two times more than those by the other method. The direct olfactory transport of Rb after IN was confirmed by-passing the blood-brain barrier (BBB), although the transportation after the other administrations was realized via BBB.

3P47: The mechanisms of gamma-ray energy conversion in water vessels

Chen, A., Tanabe, T., Yoshida, T., Sawasaki, T. (CIRSE, Nagoya University)

We propose a novel technique using special metal structures to efficiently convert γ -rays to low-energy electrons, with applications such as detoxification of water and hydrogen production using γ -ray from radioactive wastes. Using Monte-Carlo transport codes, we have studied the mechanisms of generating lower-energy photons and electrons from γ -ray in water vessels containing metal structure of various geometrical arrangements. We have demonstrated that the amount of low-energy electrons in water increases with (i) the Z number of the metal, (ii) the volume of the metal, (iii) the ability of low-energy electrons to escape from the metal and enters the water region, (iv) the closeness with adjacent metal slabs (this is dubbed the "double-mirror multiplier effect"), and (v) the ability of metal slabs to reflect high-energy photons in order to trap them within the vessel. With these basic understandings, more complicated structures were designed and compared in computer simulations. Simulation results showed that, when the relative amount of energy "wasted" in the metal region is considered, "closed-type" structures provide a better performance in terms of efficiently generating low-energy electrons in water.

3P48: Enhancement of hydrogen production by gamma-radiolysis of water

Yoshida, T.¹, Sawasaki, T.², Chen, A.¹, Tanabe, T.¹ (1.CIRSE, Nagoya University, 2.Dep. of Nucl. Eng., Nagoya University)

Gamma-radiolysis of water has been extensively studied for its importance in water-cooled nuclear reactors. The efficiency of the radiolysis of water is very low because the energy of the gamma-ray is too high to dissociate the water molecule directly. To improve the efficiency, we attempted to convert gamma-ray to lower-energy electrons and photons which were effective for chemical reactions, utilizing the interactions between gamma-ray and metals, and have succeeded in enhancing H_2 production using high Z metals. In this work, based on a separate computer simulation work, we have performed experiments of radiolysis of water sandwiched by metal slabs, and were successful in enhancing the efficiency of the radiolysis of water by controlling the thickness of metal slabs and the gap size between the slabs. Results showed that H_2 production had a maximum value when both the slab thickness and the gap size were in the 0.1mm range. Comparing with the computer simulations, the effect of lower-energy electrons on H_2 production will be discussed.

3P49: Low-Level Counting System of Ogoya Under Ground Laboratory

Hamajima, Y. and Komura, K. (Inst. of Nature and Environmental Tech., LLRL, Kanazawa Univ.)

Low-level measurements open new fields of research, such as discovery of a large number of radioactive nuclide induced by the environmental neutron, evaluation of the range and the scale of the environmental influence of a JCO flash criticality accident, and neutron flux evaluation from neutron induced radioactive nuclide that remains today. It is impossible to detect such activity with conventional massive lead shield. From 1995, our counting system has been set up at Ogoya underground laboratory (270m water equivalent) in the old

mining tunnel. This time, we start up new gamma-ray counting system of 4 well detectors, 3 planar detectors, and a coaxial detector with low-level background count-rate, with high detector efficiency, and with pure massive shield. Here, this measurement system and a communication system (remote control system from LLRL) are reported.

3P50: withdraw

3P51: Electromigration of sodium ions and electro-osmotic flow in water-saturated, compacted Na-montmorillonite

Higashihara, T., Kinoshita, K., Sato, S., Kozaki, T. (Div. of Quantum Energy Eng., Graduate School of Eng., Hokkaido Univ.)

Compacted bentonite is promising buffer material in deep-underground disposal of high-level radioactive waste. Many researchers have studied the migration behavior of radionuclides in water-saturated, compacted bentonite. In this study, the migration behavior of ^{22}Na and dissolved helium was studied in water-saturated, compacted montmorillonite under an electric potential gradient. The compacted Na-montmorillonite columns saturated with 0.1-M- NaClO_4 solutions were prepared at the dry densities 1.0 and 1.6 Mg m^{-3} . Under an electric potential gradient, ^{22}Na and dissolved helium were migrated in compacted montmorillonite by electromigration and electro-osmosis, respectively. After the migration of these chemical species, the montmorillonite specimens were sectioned into 1.0-mm-thick wafers. The concentration profiles of ^{22}Na and He were obtained by γ -spectrometry and mass-spectrometry, respectively. Based on the concentration profiles, the dispersion coefficients and dispersion length of ^{22}Na and He were determined in water-saturated, compacted Na-montmorillonite. The dispersion length of ^{22}Na was smaller than that of He. It is considered that migration path of ^{22}Na is different from that of He in water-saturated, compacted Na-montmorillonite.

3P52: Study on the solvation of trivalent lanthanoid ions in mixed solvent (DMSO/water) solutions using EXAFS

Watanabe, T., Ishii, Y. (Grad. Sch. Sci. & Tec., Shizuoka Univ.), Suganuma, H., Yanaga, M. (Fac. Sci., Shizuoka Univ.), Yaita, T., Narita, H., Tachimori, S. (JAERI)

EXAFS measurements were performed for 0.4 M LnCl_3 ($\text{Ln}=\text{Sm}, \text{Eu}, \text{Er}$ and Lu) mixed solvent (DMSO/ H_2O) solutions. The quantitative analysis of the EXAFS data has revealed (1) the variation of the solvation number in the primary solvation sphere around Ln(III) with an increase in the mole fraction of DMSO in the mixed solvent solution and (2) the variation of the average distance between Ln^{3+} and oxygen of the solvated molecules.

3P53: Coincidence Doppler broadening spectroscopy in polymer studies

Suzuki T., He C.Q., Djourelou N., Kondo K.(KEK), Ito Y. (RCNT)

Positron annihilation lifetime spectroscopy (PALS) is useful for studying intermolecular spaces, their sizes and distribution in polymers. Coincidence Doppler broadening (CDB) measurements were conducted simultaneously with the PALS measurements. The increase in the high energy part in the CDB spectrum was observed even in vacuum. The increase seemed to saturate after 300 hr measurement in vacuum. Then air was introduced in the vacuum cell. Again the small increase was observed. The increase observed after introducing air can be explained by the positron interaction with oxygen, which may be brought into polymer structures as a carbonyl group. Since the increasing rate in the vacuum and the air was similar, the oxygen effect can not be neglected even in the vacuum experiment. It can be interpreted as follows in polymer like HDPE or LDPE: air is absorbed in samples left in air; injected positrons form radicals; radicals interact with the absorbed oxygen; then carbonyl groups are

formed; positrons are attracted electronically by the carbonyl groups; then positrons interact with oxygen of carbonyl groups. Thus positrons interact electrons of oxygen.

3P54: Construction of a pulsed slow positron beam for polymer films

C.Q. He*, N. Djourelou, T. Suzuki (KEK) E. Hamada (Inst. for Env. Sci.), T. Kumaki (R&D, Hitachi), H. Kobayashi, Kenjiro Kondo (KEK), Yasuo Ito (RCNT, Univ. of Tokyo)

A pulsed slow positron beam using a radioisotope, ^{22}Na , has been constructed to apply to thin polymer films. The structure of this equipment is very simple. The time resolution of positron annihilation lifetime spectroscopy by using the pulsed slow positron beam is determined to be about 500 ps, which is sufficient to measure long-lived positron lifetime in thin polymers. Interface between a 45 nm thick epoxy thin film and the substrate of a single crystal silicon plate was investigated using the pulsed slow positron beam. The result indicates a looser interface exists between the epoxy film and the Si substrate. Surface effect on the glass transition temperature of a polystyrene film has been studied using the system. We observed that the glass transition temperatures for the subsurface layers are much lower than that in the bulk and that the glass transition temperature becomes lower near to the surface.

3P55: ^{121}Sb Mössbauer spectra of unsymmetrically substituted antimony(V) tetraphenylporphyrins.

ENDO, H., TOKUNAGA, E., TAKAHASHI, M., TAKEDA, M., AKIBA, K. (Faculty of Science, Toho Univ., Science and Engineering Research Institute, Waseda Univ.)

^{121}Sb Mössbauer spectra for unsymmetrically substituted antimony (V) tetraphenylporphyrins $[(\text{TPP})\text{Sb}(\text{CH}_3)(\text{X})]^+\text{OH}^-$ are measured to investigate the substituent effect on Sb electronic state. The observed positive quadrupole coupling constant (e^2qQ) indicates that the p electrons are much more distributed in axial direction than in the average of equatorial plane. Both isomer shift (δ) and e^2qQ are varied by changing the axial ligand X, the e^2qQ value is decreased in the order of $\text{CH}_3 \geq \text{C}_2\text{H}_5 > \text{OH} > \text{O}-\text{C}_6\text{H}_4-\text{CH}_3$, and the δ value $\text{OH} > \text{O}-\text{C}_6\text{H}_4-\text{CH}_3 > \text{C}_2\text{H}_5 \geq \text{CH}_3$. This suggests that the more electron donating substituent, the more electrons are transferred to axial $5p_z$ orbital. Furthermore, good correlations between the Mössbauer parameters (δ and e^2qQ) and the substituent parameter (σ_r) are observed.

3P56: The structure and ^{155}Gd Mössbauer spectra for Gd complex bridged by 4, 4'-bipyridyne N, N'-dioxide ligand

Suzuki, K., Kitazawa, T., Takahashi, M., Takeda, M. (Faculty of Science, Toho Univ.)

It has been recently reported that 4, 4'-bipyridyne N, N'-dioxide (dpdo) ligands and rare-earth metal ions provide interesting coordination polymer structures. We have synthesized new coordination polymers $[\text{Gd}_2(\text{NO}_3)_3(\text{dpdo})_3]\text{CH}_2\text{Cl}_2$ (1) and $[\text{Gd}_2(\text{NO}_3)_3(\text{dpdo})(\mu\text{-dpdo})]$ (2). The complexes (1) and (2) have been characterized by ^{155}Gd Mössbauer spectroscopy and single crystal X-ray diffraction determination. The Gd^{3+} for the complexes (1) and (2) have nine coordination geometry (GdO_9) consisting of nine oxygen atoms of the three nitrate ligands and the three dpdo ligands.

(Crystal Data : (1) P-1, triclinic, $a = 11.757(4)$ Å, $b = 13.098(2)$ Å, $c = 8.080(3)$ Å, $\alpha = 100.49(2)^\circ$, $\beta = 101.02(3)^\circ$, $\gamma = 86.82(2)^\circ$, $Z = 2$, $R = 0.039$, $R_w = 0.047$; (2) $P2_1/c$, monoclinic, $a = 9.474(5)$ Å, $b = 14.721(3)$ Å, $c = 17.446(4)$ Å, $\beta = 91.64(3)^\circ$, $Z = 2$, $R = 0.0590$, $R_w = 0.072$)

3P57: The distribution of heavy metal elements in clethra

Kasahara, S., Ohnishi, T., Masuko, S., Noya, Y. (Radioisotope Res. Center, Hokkaido Univ.)

We have reported as to metal elements contained some plants such as clethra, bamboo, maple etc. This time, we activated the leaf, blanch and anthotaxy of clethra and developed the

method to detect the heavy metal elements by imaging plate. We could activate the clethra leaf about 100mm square without dilapidation. Especially the picture of anthotaxy was very clear. We suppose that will be resulted from the cesium-134.

3P58:Real-time water imaging in a plant using positron emitting nuclide, ^{15}O and imaging plate

Tanoi, K., Nakanishi, T. M., Hojo, J., Suzuki, K. (University of Tokyo, NIRS)

Though water plays an important role in plant activity, water movement within the living plant tissue has not been studied in detail, mainly because the tools for the research are lacking. To get nondestructive water image in a living plant, positron emitting nuclide, ^{15}O (half-life: 2min) was produced by $^{14}\text{N}(d, n)^{15}\text{O}$ reaction, at NIRS. A soybean plant grown after 3 weeks in water culture was fixed on a vertical board and ^{15}O -water (about 2 GBq/10ml) was supplied from the root. An imaging plate (IP) was set on the board for 1 min to get water images of the plant. After acquiring the images on IP through a computer, the ^{15}O amount taken up by the plant was analyzed. Because of an extremely short half-life of ^{15}O , the experiment was carried out for 20min. After about an hour the next experiment was able to perform using the same sample, because almost of the entire radioactivity was decayed out. The water uptake amount was found to be correlated with the light intensity and water uptake was drastically reduced under high humidity.

3P59:Element Distribution within a Wood Disk by Neutron Activation Analysis

Nakanishi, T.M., Nagai, K., Hayashi, Y., Tanoi, K., Ikeue, N., Tange, T., Yagi, H., N.Nogawa

We present element profile within a wood disk (*Cryptomeria Japonica*) measured by neutron activation analysis. About 10g of wood samples collected across the annual rings were dried and burned to ash at 500°C for about 5 hours. Then the samples were irradiated by a research reactor, JRR-3M, installed at Japan Atomic Research Institute, where the thermal neutron flux was 1.9×10^{13} n/cm²/s. After 10second and 20 minute irradiations, Na, Mg, Al, K and Ca, as well as Fe and Co, respectively, were determined by γ -spectroscopy. Among the elements studied, K and Mg concentration was gradually decreased, at a constant rate, from heartwood toward sapwood, suggesting that the decrease of these elements are promising candidates to estimate the age of the wood which does not form annual rings in tropical forests. In the case of Al and Fe, the highest and the lowest concentrations were periodically found, indifferent to heartwood or sapwood. Along with element distribution, natural radioactivity, especially targeting ^{210}Pb within the disk was also studied.

3P60:The structure of new 7 coordinated uranyl complex containing the bridging ligand 4,4'-bipyridine

NISHIMURA, T., KITAZAWA, T., TAKEDA, M. (Faculty of Science, Toho University)

Uranium compounds can take various oxidation numbers; for example +3, +4, +5 and +6. The compounds containing uranyl(VI) ion (UO_2^{2+}) are most stable. The crystal structures of uranyl(VI) complexes are classified to the three groups: the octahedral structure for 6 coordination, the pentagonal bipyramidal structure for 7 coordination, and the hexagonal bipyramidal structure for 8 coordination. We have reported that a new binuclear uranyl(VI) complex consists of two 7 coordination structure which are linked through the 4-bpy bridged ligand. The formula of the new compound is $[\{\text{UO}_2(\text{acac})_2\}_2(4\text{-bpy})]$. (Crystal Data: monoclinic, $P2_1/n$ (No.14), $a = 7.720(5)$, $b = 15.996(7)$, $c = 13.969(4)$ Å, $\beta = 98.08(3)^\circ$, $V = 1707.9(1)$ Å³, $Z = 2$, $D_{\text{calc}} = 2.125$ g cm⁻³, $R = 0.048$, $R_w = 0.042$). The bond distance of U-N for 4-bpy complex (2.70(1) Å) is longer than that for reported mononuclear complex $[\text{UO}_2(\text{acac})_2\text{py}]$ (2.47(1) Å). The bond angles of uranyl group (O - U - O) were 179.0(5)° for

4-bpy complex, 173.5(8) ° for the py complex, respectively. These results show interactions between the U and N atoms for the 4-bpy complex is weaker than those for the py complex.